Visual-Quality-Driven Video Networking over 4G Wireless Broadband

Po-Han Wu

A dissertation submitted in partial fulfillment of the
requirements for the degree of:

Doctor of Philosophy

University of Washington

2014

Reading Committee:

Jenq-Neng Hwang, Chair

Payman Arabshahi

Yasuo Kuga

Program Authorized to Offer Degree:

Department of Electrical Engineering

University of Washington

Abstract

Visual-Quality-Driven Video Networking over 4G Wireless Broadband

Po-Han Wu

Chairperson of the Supervisory Committee:
Professor Jenq-Neng Hwang
Department of Electrical Engineering

This dissertation intends to develop an effective and complete cross-layer scheduling and resource allocation algorithm for real-time video camera networks over the OFDMA-based 4G mobile infrastructure. There are two main parts in our research: Visual Quality Driven (VQD) scheduling as well as resource allocation for real-time surveillance video uplink (UL) transmission, and Visual Quality Driven resource assignment for real-time video through an integrated downlink (DL) and UL system over the OFDMA-based networks.

In the VQD scheduling for video uplink, we propose an effective real-time video uplink (UL) framework for mobile wireless camera networks over an OFDMA-based infrastructure. Mobile wireless camera stations (CS) unicast their videos in real time to base stations (BS) and then these live video streams are fed to subscribers to facilitate real time video monitoring. Based on the visual quality driven utility function, the target bit rate resulting in the highest possible visual quality is quickly set for each UL video by our algorithm. To optimize the system performance, a real time video packet scheduler

and a spectral efficient resource allocation policy are derived. This scheduler is also capable of exploiting the inherent diversity gain due to channel variations. Extensive simulations demonstrate that our proposed method can significantly enhance utility, boost spectral efficiency, and stabilize the video quality.

For the integrated system, a comprehensive UL and DL framework for wireless mobile camera networks is proposed. On the UL side, this system collects unicast real-time video streams from wireless mobile camera stations (CSs) and forwards them to the social web platforms having capability to deliver live videos, such as YouTube, Twitter, Facebook, etc. On the DL side, the aggregated video streams are multicast to multiple mobile stations (MSs) to facilitate efficient distribution of these videos in real-time. Since this utility function has also taken the popularity of video contents into consideration, the number of video layers to be uploaded can be quickly determined by our resource allocation algorithm. A previously published opportunistic layered multicasting (OLM) scheduling algorithm is also applied on the DL. Simulation results prove that this proposed novel architecture of ours can significantly enhance the spectral efficiency and the users' satisfaction in both the UL and DL directions.

Table of Contents

List of Figures

List of Tables

Acknowledgements

First of all, I wish to express my deepest appreciation to my faculty advisor, Professor Jenq-Neng Hwang, for his patient guidance during my PhD pursuing years. He has always been supportive and provided me with various inspiring ideas and valuable advices as well as expert comments whenever I encountered bottlenecks while doing research.

I would also like to send my sincerest thanks to all my distinguished PhD committee members, Professor Payman Arabshahi , Professor Yasuo Kuga , Professor John Zahorjan for taking their precious time off their busy schedules to attend my final examination and make/give all the valuable suggestions and precious research/career advices.

Many thanks to Professor Yu-Hen Hu, Professor Hui Liu and Professor Brian P Otis for providing me with their expert knowledge and in-depth insightful advices and suggestions.

I am grateful to all my graduated colleagues and lab mates, Hsu-Yung Cheng, Victor Gau, and Chih-Wei Huang, and to all the previous visiting scholars to our lab, Royal Shih, Jing-Xin Wang, Hangten Wang, Shiang-Jiun Lin, Peng-Jung Wu, and Shiang-Ming Huang. They unselfishly provided me with great help along with warm friendship and shared their valuable experiences with me, especially during my very first year. Without their kindest generous help, I could never find the right working direction so as to be able to concentrate on my research work.

I thank all the present and recent members of Information Processing Lab: Chun-Te Chu, Meng-Che Chuang, Xiang Chen, Shian-Ru Ke, Kevin Lau, Kuan-Hui Lee, Pei-An Lee, Yongjin Lee, Youngdae Lee, YoungGun Lee, and Ruizhi Sun. They have made our lab such a great working place and concurrently provided me with quite a few precious research suggestions. My best wishes to all of them.

I also want to thank all my friends I have made in Seattle and all the old friends coming to visit me. Your great friendship did bring me strength and luck enabling me to reinforce my confidence and endurance to proceed further in this long rugged journey.

I am and will always be grateful to my dearest parents and family members. Their endless love and caring encouragement have been my strongest supports and fountain of energy throughout during these tough years. I fully realize that they are the greatest treasure of my life and will stay around whenever I need any guidance, supports and helps now and in the future.

Dedication

To my family

Chapter 1 – Introduction

1.1: Introduction

Recent advances in the fourth generation (4G) wireless broadband networks, such as IEEE Worldwide Interoperability for Microwave Access (WiMAX) and 3GPP's Long Term Evolution (LTE), have adopted many quality of service (QoS) enabling technologies such as orthogonal frequency division multiple access (OFDMA), single-carrier frequency division multiple access (SC-FDMA), and multi-input, multi-output (MIMO) antennas. With these technologies, 4G broadband network provides wider signal coverage and higher mobility, offers an elegant way of radio resource partition, supports QoS optimization, and has thus been considered as the most appropriate platform for wireless multimedia networking.

With these advanced wireless mobile broadband technologies and deployments of new generation wireless infrastructure, real-time video communication applications, including video uplink (UL) and downlink (DL) deliveries, are becoming very important to service providers as the source of many new business applications and also growing into the new frontiers of telecommunication industry.

However, there are still many open problems to be resolved for different video applications.

(1). Performance metrics for video networking applications: The OFDMA-based networks incorporate several QoS mechanisms to guarantee service for different

applications, including data, voice, and video. However, those QoS parameters mainly focused on PHY layer performance metrics, such as throughput and delay. Yet, these communication oriented metrics do not directly reflect the video perceptual quality experienced by users accessing the services. In general, performance metrics for video networking applications should be designed based on user experience, expectation of different applications, and network performance. [36]

(2). Resource allocation and scheduling for real-time video uplink transmission: This scenario considers multiple real-time uplink surveillance video streams over wireless channels, where the demand for high video quality and low transmission delays needs to be reconciled with the limited radio communication resources in the system and time-varying wireless channel condition of each user. The challenge we are facing is how to maximize the efficiency of aggregate video under the limited wireless uplink resource. In the real deployment, channel condition of each connection varies over time and space. Consequently, video encoding rates in different camera stations (CSs) and the modulation and coding scheme (MCS) selections of the corresponding sub-channels (SCHs) in the BS vary from camera to camera. More specifically, a user with good channel condition can upload/receive data at a higher bit rate MCS, e.g., 16 or 64QAM, compared to a user with poor channels. Therefore, when UL camera stations (CSs) with poor channel conditions are uploading high encoding rate videos through the wireless channels, they can only use lower bit rate MCS, such as BPSK, to upload their high-quality video data. The system performance will definitely be degraded due to poor radio resource usage.

Besides, each CS maintains a buffer of video packets ready to be transmitted to the BS. For real-time video services, each packet has a deadline time stamp and needs to be delivered before this deadline. Otherwise, it becomes expired and will be discarded. In other words, the video rate of each UL CS should be carefully determined according to the available resource and corresponding channel conditions, and the real-time packet scheduler should try to deliver the buffered packets on time. Thus, for efficient video UL delivery to result in optimal system performance, a mechanism comprehensively considering resource allocation, video rate adaptation, and real-time packet scheduling along with MCS selection are crucially required.

(3). Resource allocation and scheduling for real-time video multicasting : For the real-time video DL services to groups of subscribers, such as IPTV or broadcasting live events, multicast is obviously the most efficient way to deliver these applications over the resource-limited wireless networks [45]. However, the channel condition can vary considerably across the subscribers. When the video is transmitted at a lower MCS, all users can receive this video but more radio resource is consumed, which results in lower number of videos, or low encoding rate videos, can be transmitted. On the other hand, when a higher MCS is adopted for transmission, only users with good channel conditions can access this video, but those with poor channels may be starved from receiving any data. Therefore, how to effectively determine the video encoding rate and assign MCS is the main challenge when we try to optimize the performance of multicast applications.

(4). Resource allocation for real-time video transmission in the UL and DL integrated system: Recently, a new application considering the real-time video delivery over the UL and DL integrated framework has attracted a lot of attention. In this scenario, video cameras mounted on mobile devices capture the videos with live events and immediately upload the captured videos via wireless channels to a social web platforms having capability to deliver live videos, such as YouTube [73] or Facebook, for real-time sharing or distributing the video contents to groups of subscribers. For this new application, several issues arise for the network resource allocation while preserving the optimal system performance.

(a) In this integrated system, multicast should be chosen to efficiently distribute the real-time video contents to DL subscribers.

(b) As described earlier, the radio resource is limited and channel conditions of UL CSs and DL subscribers vary frequently over time and location. The video encoding rate decided on the UL side may not be the solutions to result in the highest satisfaction from video subscribers on the DL side. Thus, a resource allocation algorithm jointly considering the UL CSs' environment and DL users' requirement is indispensable.

In this dissertation, we aim to develop an effective and complete cross-layer resource allocation and scheduling algorithm for real-time unicast UL video delivery, multicast DL video distribution, and video transmission in the UL and DL integrated system over the OFDMA-based mobile infrastructure. For the real-time unicast UL video delivery, a

Visual-Quality-Driven (*VQD*) utility function is adopted as the performance metric. Based on this utility function, the target bit rate of video encoder resulting in the highest possible utility can be quickly set for each UL CS. Further, a *VQD* real-time packet scheduler considering utility, head-of-line (HOL) delay in the buffer, averaged transmitted rate of each CS, and incorporating the proposed high spectral efficient resource allocation policy are derived to reach the optimal system utility.

In the UL and DL integrated system, the layer-encoded video, such as scalable video codec (SVC) [49]-[52], is adopted to facilitate flexible and robust data rate adaptation for users under rapidly fluctuating channel conditions. Further, the utility function taking into account both the video perceived quality and the video channels' popularity is adopted as the performance metric. On the DL side, a previously proposed opportunistic layered multicasting (OLM) scheduling algorithm [13] is applied as the solution to distribute the videos to mobile station (MS) subscribers. It is capable of selecting a best subset of MS subscribers to receive a particular video layer with a view to maximizing the total utility. The OFDMA frame-based FEC code is also incorporated to enhance the robustness of multicast. On the UL side, a proposed algorithm incorporating the OLM method can quickly decide the number of video layers to be uploaded, resulting in the highest total utility, for each UL video. To optimize the system performance, a real-time UL packet scheduler is also derived. Using 4G mobile network protocols and a realistic wireless channel model, it is demonstrated through our extensive simulations that all our proposed

methods can significantly enhance utility, boost spectral efficiency, and stabilize the video quality.

1.2**: Contributions**

The contributions of this dissertation are as follows.

- To real-time video uplink system, an effective and innovative cross-layer algorithm, which comprehensively considers the video target bit rate configuration and real-time packet scheduling along with the resource allocation, is proposed. By using the proposed rate adaptation algorithm, the target bit rate resulting in the highest possible utility can be quickly set for each CS. To optimize the system performance and reach the highest possible utility, the real-time packet scheduler and a spectral efficient resource allocation policy are thus derived.
- A visual quality driven utility function, having considered the video perceived quality and the importance of video content, is formulated as performance metric of our uplink surveillance video system. This utility function is flexible and applicable with any video objective or subjective quality metrics.
- An enhanced greedy heuristic method, which focuses on maximizing the per slot and total utility, is proposed to quickly set the target bit rate for each UL video. Extensive simulation and the analysis for this algorithm are provided to demonstrate the performances.

- Our proposed real-time packet scheduling algorithm jointly considering each CS's unit utility gain, average throughput, and queuing delay, is also shown to be able to exploit the inherent diversity gain due to wireless channel variation.
- A spectral efficient resource allocation policy is derived to determine the number of slots to be assigned to a CS which is selected for uploading by real-time scheduler.
- For the integrated system, to our best of our knowledge, our proposed framework is the first one to provide the systematic solution by incorporating the UL unicast and DL multicast algorithms.
- The structure of a UL camera using layer-encoded video is clearly defined. It is proved that the UL bit streams of base and enhancement layers in CSs ought to be classified into different queuing buffers.
- To optimize the utility for DL users, the OLM scheduling [13] is employed on the DL side. With respect to uplinked video layers, the OLM selects the best subset of MSs for each video layer to maximize the total utility, and concurrently assign the most efficient MCS to transmit the data.
- The proposed UL algorithm combines the OLM method to select most suitable UL CSs to transmit more layers to optimize total utility under resource constraint conditions.
- The OLM algorithm is further applied to estimate the (i) possible number of receivers and (ii) potential utility of each video layer, deliberating the DL subscribers' channel qualities. It proves to be applicable to a real system.

1.3**: Dissertation Roadmap**

The other parts of this dissertation are organized as follows.

Chapter 2: In this chapter, we first introduce the essential concept of radio resource in the OFDMA wireless systems. Then we review the recently proposed works which are related to scheduling and resource allocation for video UL and DL transmission over the wireless networks.

Chapter 3: Our proposed systematic algorithm for a real-time video unicast uplink system is detailed in this chapter. First, the formulation of visual quality driven utility function is introduced as the performance metric. Further, the enhanced greedy heuristic method for video encoding rate adaptation is presented. The video rate resulting in the highest possible utility is quickly set for each UL video by this algorithm. To optimize the system performance, i.e., to reach the targeted bit rate and utility, a real time video packet scheduler and a spectral efficient resource allocation policy are both derived. Analyses for proposed rate adaptation algorithm and real-time packet scheduler, along with the extensive simulations will be provided to demonstrate the outstanding performance of all proposed methods.

Chapter 4: The proposed integrated UL and DL framework are presented in this chapter. We first introduce our previously published OLM multicast scheduling algorithm to serve as the solution of DL side. Moreover, in this system, the utility function that incorporates both the video perceived quality and the video channels' popularity is adopted. In order

to determine the number of video layers, which resulting in the highest system utility, for each UL video, an UL algorithm comprising the OLM method is proposed. It can be fast decide the optimal number of layers for each UL video. To optimize the system performance, a real-time UL packet scheduler is also proposed. Our integrated system comprising the OLM not only can estimate the utility to be generated for each layer in real-time, but can also select the UL CSs to transmit more layers to optimize the overall utility. In other words, a complete integrated video transmission system is constructed.

Chapter 5: The conclusion of this dissertation is presented here by summarizing our main contributions and also discussing the extension works which leads to potential research topics in the future.

Chapter 2 – Backgrounds and Related Works

In this chapter, we first introduce the essential concept of radio resource in the OFDMA wireless networks. After that, we review several recently proposed works which are related to scheduling and resource allocation for video UL and DL transmission over the wireless networks.

2.1: Radio Resource in OFDMA-based Mobile Network

2.1.a Subchannel and Slot Composition in WiMAX OFDMA Frame

For OFDMA systems, such as IEEE 802.16e WiMAX, the radio resource is organized into OFDMA frame structure, as shown in Figure 2.1, and allocated in both frequency and time domains. In the frequency domain, the subcarriers are grouped to form sub-channels (SCHs) according to different permutation schemes. In particular, the band adaptive modulation and coding (AMC, or band-AMC) scheme groups connect subcarriers (eight data subcarriers and one pilot subcarrier) with a frequency bin, as shown in Figure 2.2. One, two, or three adjacent frequency bins over respectively six, three, or two consecutive OFDM symbol frames in time form a slot, which is the basic unit of radio resources that may be assigned to any specific user (in this case, a CS). AMC permutation enables multi-user diversity by choosing the SCH with the best frequency response and is adopted for UL in this work. Besides, in [27] and [28], the OFDMA frame duration is set to 5 ms and the channel coherence time is also assumed to be 5 ms [28].

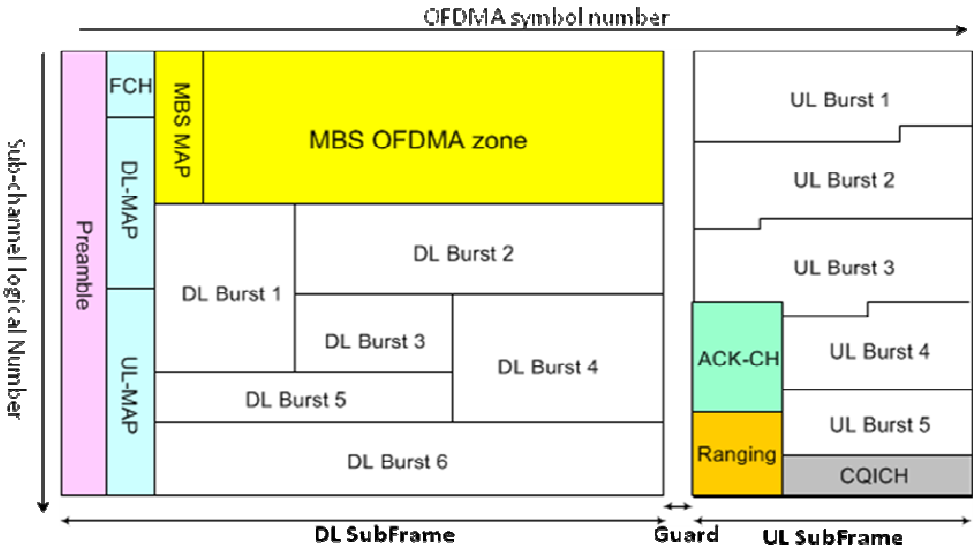

Figure 2.1: WiMAX OFDMA TDD Frame Structure

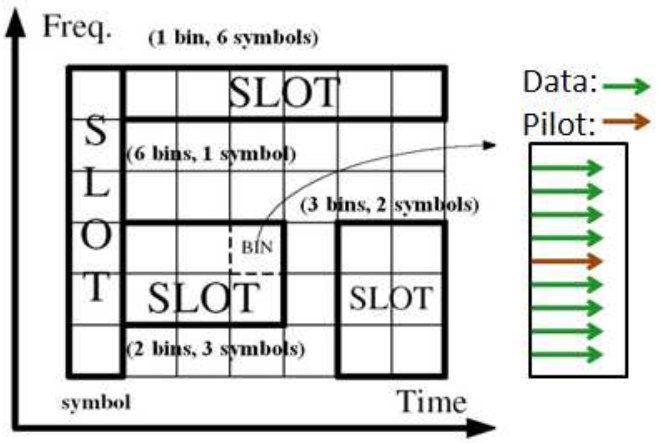

Figure 2.2: Time-Frequency Slot Structure in WiMAX OFDMA Band-AMC Mode

Another commonly used scheme is the diversity permutation. It pseudo-randomly draws the subcarriers to form a SCH in frequency domain and thus provides better frequency diversity so that the channel quality are less likely to be affected by frequency

selective fading. It is also called partially used subcarrier (PUSC) mode and is adopted for DL in our work.

2.1.b Video over Multicast and Broadcast Service in WiMAX

In WiMAX, multicast is operated by a central base station (BS) direction to the mobile stations (MSs) within a cell sector to listen in to a particular slot. In order to support the multicast and broadcast services (MBS), the WiMAX standard specifies a space-time coding (STC) zone, called MBS OFDMA zone, within each DL frame [27]. Each MBS zone shall consist of several sub-channels in the frequency domain and several OFDM symbols in successive time intervals. All resources within this zone are dedicated to multicast service. As shown in Fig. 2.1, the MBS zone may either share the DL frame with other uni-cast services, or may occupy the entire DL frame. The radio resources within the MBS zone are also partitioned into slots. A slot is the minimum granularity data allocation unit in an OFDMA frame, as already described in the previous section. The total number of slots within each sub-channel in the MBS zone is predetermined and cannot be changed.

For the video DL multicast in this dissertation, we focus on how to assign the resources in a MBS OFDMA zone. Since the MBS zone is dedicated to the multicast traffic, other types of traffic will not be considered.

2.1.c Modulation and Coding Schemes in IEEE 802.16e WiMAX

A slot may be modulated at one of M different rates $\{C(m); 1 \leq m \leq M\}$ according to a specific MCS m (see Table 2.1). For IEEE 802.16e [20], $M = 7$, and $C(m)$ = [9.6 14.4 19.2 28.8 28.8 38.4 43.2] Kbps/slot, $m=1,2,\ldots,7$. The total amount of radio resource is limited to G_0 slots per OFDMA UL frame. The modulation rate is chosen to ensure the bit error rate (BER) is kept below a preset SNR threshold (TH) for a given channel quality index (CQI). Thus, given a CQI (b(t)), the corresponding highest possible modulation rate, noted as $m(b_{(t)})$, can be uniquely determined. CQIs are frequently estimated by the BS based on received pilot subcarriers. Due to fast and slow fading, the CQIs between a CS and the BS vary over different frequency bands. In this dissertation, we use the normalized capacity *b(t)* to serve as a good approximation to the instantaneous CQI at time *t* when a specific MCS is chosen, as shown in Table 2.1.

Table 2.1: MCS (m), Slot Capacity (C), and Normalized Capacity (b) in **[20]**

Type (***m***)	Modulation and Code Rate	SNR TH (dB)	Capacity (***C*** :Kbps/slot)	Normalized Capacity ***(b)*** (bits/subcarrier)
1	**QPSK 1/2**	**5**	**9.6**	**1**
2	**QPSK 3/4**	**8**	**14.4**	**1.5**
3	**16 QAM 1/2**	**10.5**	**19.2**	**2**
4	**16 QAM 3/4**	**14**	**28.8**	**3**
5	**64 QAM 1/2**	**16**	**28.8**	**3**
6	**64 QAM 2/3**	**18**	**38.4**	**4**
7	**64 QAM 3/4**	**20**	**43.2**	**4.5**

2.2**: Related Works**

2.2.a Resource Allocation and Scheduling for Real-Time Unicast Video Uplink System

To overcome the hurdles of deploying wireless real-time video uplink systems discussed in Sec. 1.1-(2), the scheduling and resource allocation scheme plays a crucial role. Round robin (RR) [24] is a simple scheduling algorithm but commonly adopted in the practical wireless system to fairly assign the resource one by one to all connections. However, it cannot satisfy various service requirements from different wireless users. Thus, Weighted Round Robin (WRR) [42][43] and Weighted Deficit Round Robin (WDRR) [44] have been applied for scheduling in uplink direction. Both methods still allocate the resource one by one but the number of allocated resource may be determined based on their predefined weights. The weights can be related to queue length, packet delay, or the number of slots [43][44] and may be dynamically changed over time. WDRR can further avoid the issue of missed opportunities by using the deficit Counter (dc), which records the number of slots to be assigned to each user in each round. If the value of dc is too small to allow one packet to be uploaded, then this dc value will be saved for the next round. The main advantage of these RR variations is their simplicity so that is easy to be implemented, but we cannot influence the serving order and do not consider each user's channel condition for the scheduler of this type. In the wireless networks, there is a possibility to explicitly assign the slots to some connections in urgent need, thus needing to specify the serving order. Although changing the serving order

makes scheduling more complicated, it allows the system to control the maximum delay and jitter values.

Many cross-layer (PHY and MAC layers) QoS-guaranteed scheduling schemes for IEEE 802.16 (WiMAX) systems have been reported in [3]-[7]. These methods generally evaluate serving priority by jointly considering all connections' channel conditions and QoS requirements. The method proposed in [3] requires a significant overhead for a low-power mobile station (MS) to upload status information, such as delays of all packets and requirements of bandwidth [7]. Several efficient user/connection based schemes have subsequently been proposed and claimed to be more suitable for UL scheduling [4]-[7]. The proportional fair scheme (PFS) [8] has been widely used in mobile networks with the objective of maximizing the long-term fairness and throughput. However, it has no mechanism to guarantee the QoS for real-time services. Later, an improvement is proposed in [9] that jointly considers PFS, capacity prediction, and video rate adaptation to support the QoS requests of UL videos. Well-known scheduling strategies, such as M-LWDF and EXP [10]-[12], facilitate real time video streaming by guaranteed minimum throughput and enhanced MS priority scheduling.

In order to achieve high video quality for real-time video streaming over the mobile 4G network, it is necessary to adaptively adjust the target bit rate of the video encoder based on actual wireless network status, such as frequently changing error-prone wireless channel condition or delays resulting from network congestion. However, not all resource allocation works consider this issue. The work in [4] concentrates on supporting

QoS by real-time scheduling and transmission rate assignment, i.e., the number of packets to be delivered in each OFDMA frame, which is determined based on each user's instantaneous channel quality and the number of slots assigned. It only considers constant bit rate (CBR) application without rate adaptation mechanism. Similar situation can be seen in [3][5][6]. An adaptive rate control for real-time video over 802.16e network by observing each CS's average throughput fluctuation is provided in [46]. When the average throughput is stable and above a predefined threshold, it implies that the network bandwidth is sufficient and the video encoder can be adjusted to a higher bit rate. Otherwise, the bit rate should be adjusted lower because the network is congested. In [47][48], a method which first estimates the possible capacity of each CS, then scaling the encoder’s target bit rate based on the observed packet loss rate is proposed for WLAN system. The work in [9] extends the concept in [47][48] to the system in 4G network by jointly considering PFS scheduler, fair resource allocation, capacity prediction, and packet loss rate and proposes a cross-layer solution for QoS-guaranteed video uplink system. These existing works focused on QoS parameters in PHY layer performance metrics, such as packet loss rate, throughput, and jitter. Yet, these communication oriented metrics do not directly reflect the perceptual quality experienced by the subscribers.

Recently, the perceived quality of video networking applications, commonly formulated as a utility function to be optimized, has been promoted as a more appropriate performance metrics for wireless video streaming [13]-[16]. These works focused on the

downlink (DL) radio resource allocation problems. The greedy method in [16] has been extended to the scenario of uplink video scheduling [17][18]. However, these algorithms do not scale-up well with increasing users due to the need of tracking resource and utility variations. In [19], a framework for joint DL and UL real-time mobile video transmission in a wireless camera network (WCN) is proposed. The videos from UL CSs are scheduled according to the feedback of quality of experience (QoE) aggregated from all DL multicast MSs.

2.2.b Resource Allocation for Integrated Downlink and Uplink Real-Time Scalable Video System

As described in Sec. 1.1-(3) and (4), multicast is the most efficient way to deliver the video streams to group of mobile subscribers (MSs) over the wireless networks [45], and thus is adopted as the DL solution in our integrated system. With such a service, groups of MSs on the DL side can view popular video programs at real time while roaming around metropolitan regions.

The inclusion of wireless multicast and broadcasting services in the WiMAX standard [20][27] offers great promises to provide real-time video multicast services, such as IPTV, over WiMAX channels [53]-[57]. Recently, several works on multicast service over 802.16 have been reported. In [58] and [59], an overview of how multicast/broadcast services (MBS) are supported over the WiMAX standard is proposed. The analysis for the protocol structure in case of video/IPTV delivery is also introduced in [60]. In [53], a

two-level superposition coded multicast service is proposed. The video data is partitioned into basic quality data and enhanced quality data and both are transmitted albeit at different rate. The goal is to ensure subscriber stations (SS) can at least receive basic quality data even at bad channel condition. No resource allocation issue is considered in this work. Some optimal resource allocation algorithms for the layered video delivery on the internet were proposed [59][61]. However, without consideration of adaptive MCS, they cannot be adopted in a wireless scenario. In [54], SVC is incorporated and every subscriber is guaranteed to be served with *compulsory* layers of videos. With remaining radio slots in the MBS zone, the video program and layer that maximizes a *marginal utility* measure will be chosen. The dependency between base layer and enhancement layer in SVC is not explicitly exploited in this approach. In [55], the base layer is transmitted in a MCS that maximizes the number of receivers. Subsequent enhancement layer videos are assigned based on a similar heuristic criterion of maximizing marginal utility. *Fairness* is imposed by using the logarithm of the MCS rate as the definition of a utility function. A constraint on feasible rate to assign is imposed based on the dependency of enhancement layer video to the base layer video.

Recently, the concept called opportunistic multicast scheduling [62] has attracted growing attention. In contrast to opportunistic unicast scheduling [8], which schedules the best subset of users in each transmission to receive different content separately, opportunistic multicasting schedules the best subset of users in each transmission to receive the same content. The works in [63] and [64] further show that the throughput

capacity of opportunistic multicasting can be further improved by collaborating with forward error correction (FEC) codes, and the throughput can be further improved when temporal optimization across scheduled frames is conducted. Authors in [65] propose an opportunistic scheduling algorithm based on fixed rate of FEC code and throughput requirement per resource unit.

For the scheduling and resource allocation on the UL side, many works, including the QoS-guaranteed and visual quality driven algorithms, have been introduced in Sec. 2.2.(a). As for UL and DL integrated system, the utility function reflecting the perceived quality of video subscribers, i.e., the satisfaction level of the subscribers' access to the service, is adopted as the performance metric for this system. Existing works [13]-[16] incorporating perceived visual quality as part of the utility function for multimedia communication are mainly focusing on the downlink radio resource allocation problems. The greedy method in [16] is extended to the scenario of uplink video [17][18]. Authors in [17] also consider the video's popularity from subscribers on the DL while allocating resource to each UL video. The unicast scenario is applied for DL subscribers. The work in [18] proposes a SVC upstream system including live and on-demand videos. and its focus is on solving the resource allocation problem inside each UL camera.

Chapter 3 –Resource Allocation for Real-Time Surveillance Video Uplinking over OFDMA-Based Wireless Networks

3.1 Overview for Real-Time Surveillance Uplink Video System

Wireless or mobile surveillance systems that integrate wireless cameras or ad-hoc wireless video sensor networks with moving vehicles or mobile devices have become reality [1], [2]. As shown in Figure 3.1, video streams captured by wireless or mobile camera stations (CSs) are uploaded via uplink (UL) wireless channels to a control center where the acquired videos can be archived, analyzed and/or distributed.

Surveillance systems of this kind have numerous applications, including real time traffic monitoring, facility monitoring, combat/rescue operation monitoring, disaster relief and damage assessment, etc. Depending on specific application scenarios, different quality of service (QoS) requirements may have to be imposed on the design of such systems. For example, video streams that report critical unfolding events will require high QoS levels compared to streams that contain no events.

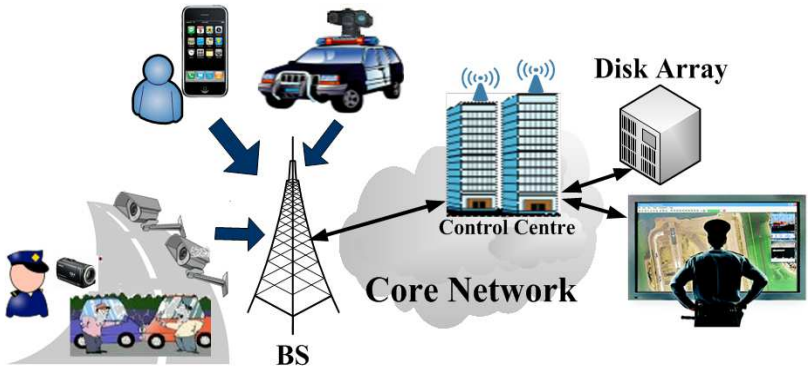

Figure 3.1: Real-time video surveillance system over mobile networks

In this chapter, we consider the scenario where multiple live surveillance videos, from either fixed or mobile CSs, compete for wireless channels to upload their videos to the BS. The key innovation of this framework is to use visual quality driven utility function to decide how the long-term UL video bit rate and the real-time UL radio resource are to be assigned.

In a realistic wireless environment, the radio spectrum is limited and the channel conditions of UL CSs vary frequently over time and space. For efficient video uplink delivery in a WCN, the target bit rate for all CSs should be decided according to the available resource and corresponding utility. Furthermore, service scheduling and modulation coding scheme (MCS) should be chosen to facilitate real-time delivery. Based on these settings, UL resource allocation problems are formulated and optimized in this chapter. There are 2 key objectives of this work: 1) In order to maximize the system utility, a long-term encoding rate assignment problem has to be formulated to decide the target bit rates for all CSs. Towards this goal, a fast and effective visual quality driven algorithm is proposed to quickly obtain the best utility and bit rates for all CSs. The complexity and approximation analysis results of this algorithm indicate that the solution is in a close proximity to the optimum and can be achieved in polynomial time. 2) In order to achieve each CS's target utility and bit rate obtained from the first objective, a real-time scheduling problem needs to be solved. Towards this goal, a utility-based priority function which is able to exploit the diversity gain embedded in channel variations is designed as the scheduler. By incorporating it in the proposed slot

assignment policy, not only each CS can achieve its target utility and bit rate, but also can the system improve its overall throughput. Advantages of the proposed algorithms for both objectives 1) and 2), including some 80% more enhanced utility, extremely low packet loss, much higher throughput, and more stable video quality, are all demonstrated in simulations utilizing the realistic wireless channel model and the 4G network protocol parameters.

3.2 **Resource Management Problem for Real-time Uplink Video**

In this chapter, UL resource allocation problems are formulated and optimized by 2 key steps. 1) In order to maximize the system utility, a long-term encoding rate assignment problem has to be formulated to decide the target bit rates for all CSs. 2) Since each CS's target bit rate along with the target utility are determined in 1), to achieve each CS's target, a real-time scheduling problem needs to be solved. We will describe and formulate the objectives 1) and 2) in subsection 3.2.a and 3.2.b respectively.

3.2.a Long-Term Video Rate Assignment Problem

Assume V video streams, each captured by a CS, are to be uploaded to the control center via OFDMA-based wireless uplinks. Each uploading video is assigned a target bit rate by the BS from L different encoding rate modes. More specifically, we denote $\mathbf{R}_0=[R_{v,l}]$ (in bps) to be an $L \times 1$ vector consisting of the L allowable target bit rates, e.g., $\mathbf{R}_0$= [500 700 1000 1200] ^{T} Kbps, $l=1,\ldots,4$, and each CS needs to be assigned a bit rate from $\mathbf{R}_0$ for uploading. Further, we define an *$1 \times L$ assignment vector* $\mathbf{a}_v = [a_{v,l}]$. If the v^{th}

CS is assigned with the l^{th} rate mode, $a_{v,l}$ is set as 1 and other elements in $\mathbf{a}_v$ are all 0. Thus, the bit rate assigned to the v^{th} CS, noted as R_v , can be expressed as:

$$R_v = \mathbf{a}_v \mathbf{R}_0 = \sum_{l=1}^{L} a_{v,l} \cdot R_{v,l} \ . \tag{3.1}$$

For long-term bit rate assignment, the average CQI of each CS over a longer period of time (e.g., for couple seconds in a real-time application) is required. In this work, the average CQI of the v^{th} CS up to time t, i.e., $b_v^{avg}(t)$, is evaluated using an exponential window:

$$b_v^{avg}(t) = (1-\rho) \cdot b_v^{avg}(t-1) + \rho \cdot b_v(t), \tag{3.2}$$

and ρ is empirically set as 1/50 for real-time services [21],[22].

Now we define the average slot capacity $C_v^{avg}(t) = 9.6 * b_v^{avg}(t)$ Kbps/slot [20], as shown in Table 2.1. This value is instrumental in the task of estimating the average slots required when a bit rate $R_{v,l}$ (Kbps) is assigned to a CS by the BS. For the l^{th} bit rate mode, the average number of slots required is $G_{v,l} = \lceil R_{v,l} / C_v^{avg} \rceil$. Thus, the average number of slots needed by the v^{th} video stream is expressed as:

$$G_v = \sum_{l=1}^{L} a_{v,l} \cdot G_{v,l} \ . \tag{3.3}$$

In OFDMA, the total number of slots available at each OFDM burst is caped at G_0 slots. Hence, the radio resource constraints can be represented by (3.4):

$$\sum_{v=1}^{V} G_v = \sum_{v=1}^{V} \sum_{l=1}^{L} a_{v,l} \cdot G_{v,l} \le G_0 . \tag{3.4}$$

The utility function of networking applications in general should directly tie together expectations to applications and user perception [36]. In the video uplink systems, for the purpose of qualitative analysis, a common approach is to represent the utility as a function of both video quality metrics and subjectively calibrated parameters [17][32]. The calibrated parameters can be assigned by different criterion[23][32] of applications. In this work, we assign a weight factor w_v to reflect the importance of a video which is a situation-dependent subjective criterion that ties closely to visual quality perception of surveillance systems. For example, a video showing an emergency event should have a higher priority, i.e., higher w_v, than other videos. Further, we define $u_{v,l}$ to be the video quality if the v^{th} video stream is assigned to the l^{th} bit rate, where $u_{v,l} > u_{v,l-1}$ and $u_{v,l}$ can be directly tied to the subjective or objective quality metrics. In the simulations of this paper, we use peak signal to noise ratio (PSNR) to approximate the values of $u_{v,l}$ because of its simplicity and low complexity [38][39] for UL CSs and reasonable degree of correlation with subjective video quality [33][34], so that it can also be translated to subjective metrics, e.g., mean opinion score (MOS), using various methods when needed [33][40][41]. In line with these discussions, the overall utility function for long term uplink bit rate assignment can be expressed as:

$$U = \sum_{v=1}^{V} w_v \cdot \left(\sum_{l=1}^{L} u_{v,l} \cdot a_{v,l} \right) = \sum_{v=1}^{V} U_v, \tag{3.5}$$

where U_v is the long term utility to be generated by v^{th} CS.

Eqs. (3.4) and (3.5) lead to the following problem formulation:

P1. A Long Term Bit Rate Assignment Problem

Given $\mathbf{R}_0$, w_v, b_v, *and* $u_{v,l}$, *find the assignment* $\mathbf{a}_v = [a_{v,l}]$ for all CSs *that maximizes the total long term utility U defined in* (3.5). *This can be expressed as:*

$$\max\ U = \sum_{v=1}^{V} U_v\ ,$$

subject to the constraints in (3.4) *and*

$$\sum_{l=1}^{L} a_{v,l} = 1, \quad 1 \le v \le V. \tag{3.6}$$

It implies that each CS will be assigned to a designated bit rate, i.e., at least the lowest rate has to be assigned to a CS to ensure the minimum quality for each UL video because of the nature of surveillance applications. The solution to **P1** is the assignment $\{\mathbf{a}_v^*\}$ for all V CSs. It will then be substituted into (3.1) to calculate the optimal bit rate assignment for each CS as:

$$R_v^* = \mathbf{a}_v^* \mathbf{R}_0 = \sum_{l=1}^{L} a_{v,l}^* \cdot R_{v,l}\ .$$

Further, the video quality assignment, i.e., the targeted video quality, for each CS can be noted as:

$$u_v^* = \sum_{l=1}^{L} a_{v,l}^* \cdot u_{v,l}. \tag{3.7}$$

Thus, the targeted utility of each CS can be expressed as

$$U_v^* = w_v \cdot u_v^*\ .$$

Problem P1 (Eqs. (3.4) and (3.5)) is the classical 0-1 knapsack problem with additional constraints described in (3.6), which has the worst case complexity L^V.

3.2.b Real-Time Packet Scheduling Problem

Solution to problem P1 yields an optimal targeted average bit rate assignment R_v^* and an optimal targeted utility U_v^* for each CS. In order to achieve the targeted U_v^* and R_v^*, an effective packet scheduler is essential. The video streams are allocated with G_v^* slots in each OFDMA frame. However, bit rate assignment does not bind the CS to any particular slot of any specific SCH (frequency band). Besides, for live video streaming, each packet has a deadline ($D_{v,max}$) and should be delivered before the $D_{v,max}$. Otherwise, it will be discarded and resulting in utility degradation. Thus, to achieve the U_v^* obtained from P1, the objectives of real time packet scheduling is to assign slots to each CS such that (a) the real time constraints are met, and (b) the average bit rates will be as close to those assigned bit rates as possible.

For a particular OFDMA frame, CQIs between the CSs and the BS vary among SCHs. This information is represented by $b_{v,k}$, the number of bits that a subcarrier can be transmitted if the k^{th} SCH is assigned to the v^{th} video stream.

In an OFDMA UL sub-frame, there are G_0 slots and K SCHs. Thus, each SCH has $G_0/K = G_K$ slots. The task of the BS is to assign SCHs and the number of slots in each SCH to each of the V video streams. Define $S_{v,k}$ is the number of slots in the k^{th} SCH allocated to the v^{th} video stream at the current UL sub-frame. Summarizing above notations, for the v^{th} CS, the number of bits that are allocated at the t^{th} OFDMA frame can be expressed as:

$$r_v(t) = \sum_{k=1}^{K} S_{v,k} \cdot (b_{v,k}(t) \cdot scr),$$

where *scr* is the number of data subcarriers in each slot. Also, for the k^{th} channel,

$$\sum_{v=1}^{V} S_{v,k} \le G_K \,. \tag{3.8}$$

Each CS maintains a buffer of video packets ready to be transmitted to the BS. For real time video streaming, each packet has a deadline ($D_{v,max}$) time stamp. If the packet is not delivered before the deadline, it becomes expired and will be discarded. Packets in the buffer can be divided into two categories: time critical vs. time less-critical. Time critical packets, with its size denoted by $r_{v,c}(t)$, have pressing deadlines and must be transmitted immediately. Otherwise, utility of the upload video will be compromised, diminishing the utility value due to the packets discarded. Less-critical packets have more relaxed deadlines, and may remain in the buffer for a short while without causing utility reduction if resource is insufficient then. Clearly, it is desired that

$$r_v(t) \ge r_{v,c}(t) \ge 0, \tag{3.9}$$

where $r_v(t)$ is the actual number of packets (bits) of the v^{th} video that are transmitted at time *t*. The quality generated by the uploaded $r_v(t)$ can be noted as $\hat{u}_v(t)$. If the actually assigned bit rate $r_v(t) < r_{v,c}(t)$, then the overall utility value will be reduced by a non-negative amount $\alpha_v(t)$ for failing to meet the real time constraint, which can be shown as

$$\alpha_v(t) = w_v \cdot \left(u_v^*(t) - \hat{u}_v(t)\right),$$

where u_v^* is as defined in (3.7).

Now we define the indicator function $J(a, b) = 1$, if $a>b$; otherwise, $J(a, b)=0$. Then the penalty of utility value discussed above may be expressed as

$$\alpha_v(t) \cdot J\left(r_{v,c}(t), r_v(t)\right).$$

As for less-critical packets, they should be transmitted if there are still slots available after all critical packets are allocated. Above discussions lead to a cost function at time t :

$$E(t) = \sum_{v=1}^{V} \alpha_v(t) \cdot J\left(r_{v,c}(t), r_v(t)\right). \tag{3.10}$$

More specifically, the reduced utility is the difference between the targeted utility and the generated utility. The packet scheduler has to make the utility uploaded by each CS be as close to U_v^* as possible so that the utility reduced can be minimized.

Now we are ready to present the problem formulation:

P2. A Real Time OFDMA Slot Assignment Problem

Find $S_{v,k}$ *for each* (v, k) *such that* $E(t)$ *in* (3.10) *is minimized, which is formulated as*

$$\min E(t),$$

subject to constraints (3.8) *and* (3.9).

In our work, after P1 is solved, any procedure applied to P2 is to reach the targeted U_v^* found in P1 and will not change the determined P1 solution; therefore, the optimization of P2 is regarded as a finer search of detailed parameters.

In a mobile network, it is difficult to allow UL users to upload all their packet information to the BS due to the fact that the resource for feedback is limited. Thus, a BS actually cannot have all the information from CSs for UL scheduling [7][9]. Because of this, the feedback information used in our solution to P2 along with its practical availability in a BS is considered as follows. For 802.16 and LTE, the number of critical

Table 3.1: List of Notations

Notation	Description
v	Index of a UL video/camera station (CS)
l	Index of encoding rate mode in a video
L	Total encoding rate modes in each video
$R_{v,l}$	Target bit rate (Kbps) for l^{th} mode of v^{th} video
R_v	target bit rate (Kbps) assigned to v^{th} CS
$u_{v,l}$	video quality when $R_{v,l}$ is adopted
$\eta_{v,l}$	incremental unit utility from $(l\text{-}1)^{th}$ to l^{th} mode
G_v	Avg. number of slots needed to UL v^{th} video
G_0	Total available slots for UL in an OFDMA frame
b_v	Channel quality (CQI) of v^{th} CS
$r_v(t)$	Bits allowed to be uploaded by v^{th} CS at time t
$S_v(t)$	number of slots assigned to v^{th} CSs at time t
$R_{v,min}$	Minimum reserved rate for real-time video
$D_{v,max}$	Tolerable delay for real-time video packet
$\tau_v(t)$	HOL delay in v^{th} CS at time t

packets and the total number of packets in the buffer (queue length) can be reported by CSs to the BS via the information of bandwidth request and buffer status through the control channel [24]-[26]. Further, head of line (HOL) delay $\tau_v(t)$, i.e., the waiting time of the first packet of the v^{th} video in the transmit buffer, is used to determine if a CS has critical packets. The $\tau_v(t)$ must be lower than the highest allowable delay $D_{v,max}$ to prevent packets from being dropped. It can also be fed back to the BS via control channel [4][25]. The notations used are summarized in Table 3.1 for readers' convenience.

In this chapter, a cross layer algorithm, called Visual Quality Driven (*VQD*) Scheduling, is proposed to solve **P1** and **P2**. As shown in Figure 3.2, this systematic method intelligently considers the interaction between the APP and MAC/PHY layers to search the optimal solutions for **P1** and **P2**. Further discussions for *VQD* are detailed in the following Sections 3.3 and 3.4.

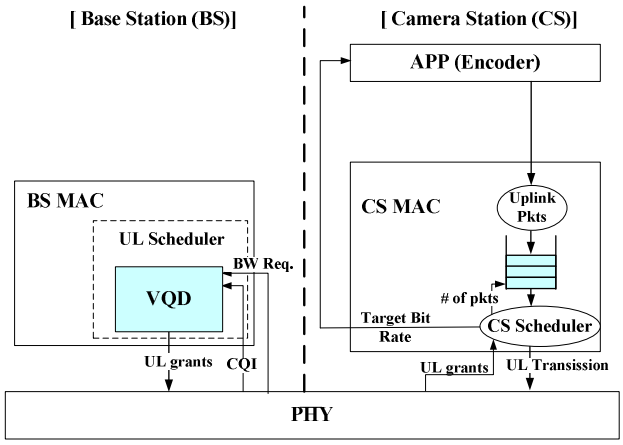

Figure 3.2: VQD System: In BS, the VQD module is for optimal UL utility

3.3 Long-Term Video Encoding Rate Adaptation and Resource Allocation

3.3.a Long-Term Uplink Bit Rate Assignment

To solve the problem of **P1**, we first define per-slot utility gain $\phi_{v,l} = w_v u_{v,l} / G_{v,l}$, and rewrite (5) as follows:

$$U = \sum_{v=1}^{V} \sum_{l=1}^{L} G_{v,l} \cdot \phi_{v,l} \cdot a_{v,l}, \tag{3.11}$$

where $\phi_{v,l}$ is the unit utility gain when video stream v is assigned with bit rate #l. Denote U_{max} to be the maximum utility that can be achieved with G_0 or fewer slots. Clearly, the per unit utility gain U_{max}/G_0 will also be the largest. This observation leads to the first two steps of the bit rate assignment heuristic algorithm. To obtain the optimal utility gain, we introduce the notion of incremental utility. For a video stream, the change of utility value due to change of bit rate levels from l–1 to l is noted as $\delta U_{v,l} = w_v(u_{v,l} - u_{v,l\text{-}1})$, and the

change of slot demand is $\delta G_{v,l} = G_{v,l} - G_{v,l\text{-}1}$. Thus, one can define the incremental unit utility gain as

$$\eta_{v,l} = \frac{w_v \left(u_{v,l} - u_{v,l-1}\right)}{G_{v,l} - G_{v,l-1}} = \frac{\delta U_{v,l}}{\delta G_{v,l}}; \quad 1 \le l \le L \ , \tag{3.12}$$

where $u_{v,0}$ and $G_{v,0}$ are both defined as zero. Then the algorithm proceeds with bit rate assignment as follows.

Step 1. Compute and then sort $\{\eta_{v,l}; 1 \le v \le V, 1 \le l \le L\}$ to yield a mapping of index (v, l) to an ordered list $\{(v'(f), l'(f)); 1 \le f \le F\}$ such that

$$\eta_{v'(1),l'(1)} \ge \eta_{v'(2),l'(2)} \ge \cdots \ge \eta_{v'(F),l'(F)},$$

where f is the rank index for ordered list and $F = V \times L$.

Step 2. Set $G_u(0) = 0$.

For f= 1 to F,

Compute $G_u(f) = G_u(f-1) + G_{v'(f),l'(f)}$

If $G_u(f) \le G_0$,

set $a_{v'(f),l'(f)} = 1$ and $a_{v'(f),l'(f)\text{-}1} = 0$, if $l'(f)\text{-}1 > 0$

Else $G_u(f) = G_u(f-1)$

$J = f - 1$, then break the for loop

End for loop

Step 3.

For $f^* = J+1$ to F,

If $\delta U_{v'(f^*),l'(f^*)} > \sum_{f=1}^{J} \delta U_{v'(f),l'(f)}$

(i) reset $\{a_{v'(f),\,l'(f)} = 0\ ,\ G_u(f)=0\ ;\ 1 \le f \le J\}$

(ii) set $a_{v'(f^*),l'(f^*)} = 1$

(iii) Redo ***Steps***1 and 2 for the rest (v, l) with $G_u(0) = G_{v'(f^*),l'(f^*)}$

End for loop

If $G_u(J) < G_0$, perform ***Steps*** 4 and 5. Otherwise, exit.

With the ***Steps*** 1 and **2** in this greedy heuristic, each video stream is assigned with the most efficient transmission bit rate in terms of utility value per slot, starting from the most efficient video stream. Note that not all video streams may be assigned with a bit rate. ***Step 3*** guarantees the algorithm performance by preventing any extremely high utility video, but with lower per slot usage, from being discarded.

On the other hand, it is possible that $G_u(J) < G_0$. In this situation, even each video stream is assigned a bit rate that has maximum unit utility gain, there might be still slots left. Hence, it is possible to transmit some videos at even higher bit rates to maximize the overall utility. To do this, one may apply selection procedures as ***Steps 3*** and ***4*** to select the video streams to transmit at higher rates. More specifically,

Step 4. Find each CS's mode by $l^*(v) = \arg\max\{a_{v,\,l}\ ;\ 1 \le l \le L\ \}$ and then sort $\{\delta U_{v,\,l^*(v)}\ ;\ 1 \le v \le V\ \}$to yield a mapping of index v to an ordered list $\{v^*(q);\ 1 \le q \le V\}$ with rank index q so that

$$\delta U_{v^*(1),l^*(v^*(1))} \le \delta U_{v^*(2),l^*(v^*(2))} \le \cdots \le \delta U_{v^*(V),l^*(v^*(v))}.$$

Next, for all non-selected higher modes # ($l^*(v)$+1), where $1 \le l^*(v)+1 \le L$,

sort $\{\delta U_{v,\, l^*(v)+1};\ 1 \le v \le V\}$ to yield a mapping of index v to an ordered list $\{v''(q'');\ 1 \le q'' \le V\}$, such that

$$\delta U_{v''(1),\, l^*(v''(1))+1} \ge \delta U_{v''(2),\, l^*(v''(2))+1} \ge \cdots \ge \delta U_{v''(V),\, l^*(v''(V))+1}\ .$$

Step 5.

For q'' = 1 to V,

For q = 1 to V,

Compute $\delta G = \delta G_{v''(q''),\, l^*(v''(q''))+1} - \delta G_{v^*(q),\, l^*(v^*(q))}$

If $\delta U_{v''(q''),\, l^*(v)+1} > \delta U_{v^*(q),\, l^*(v^*(q))}$ && $G_u(J)+\delta G \le G_0$,

set $a_{v''(q''),\, l^*(v''(q''))+1} = 1$ and $a_{v''(q''),\, l^*(v''(q''))} = 0$.

$a_{v^*(q),\, l^*(v^*(q))} = 0$ and $a_{v^*(q),\, l^*(v^*(q))-1} = 1$.

$G_u(J) = G_u(J)+\delta G$

Then redo Step 4 and 5.

End if

End for

End for loop

3.3.b Analysis for VQD Algorithm to Solve P1

We now provide an analysis of *VQD* algorithm proposed for long-term bit rate assignment. As described in Section 3.2.a, the **P1** is closely related to the 0-1 knapsack

problem and is NP-hard. In general, the method to optimize unit resource usage, known as the greedy heuristic method, can potentially result in poor performance for 0-1 knapsack problem. Thus, we first show that our proposed algorithm can at least guarantee 1/2-approximation in this type of problem.

Theorem 1. *For long-term resource allocation, the VQD can at least achieve the 1/2–approximation of optimal performance for a 0-1 Knapsack problem.*

Proof: Please refer to Appendix A1.

Theorem 1 gives a loose lower bound for the *VQD* algorithm in this 0-1 knapsack problem. In the *VQD*, we assign bit rate according to δG, which is the slot demand when bit rate is increased from $(l-1)^{\text{th}}$ to l^{th}. By keeping this δG small (as in comparison with G_0) and iteratively allocating this small portion of resource to CSs while deciding their bit rates, the performance of *VQD* can be further enhanced. More specifically, define

$$\varepsilon = \max_{v,l}(\delta G_{v,l} / G_0) \ ,$$

where ε denotes the maximum ratio of slots demand for higher bit rate over total slots for uplink. Then a stronger performance bound that *VQD* can provide within a factor of *(1-ε)* of the optimal solution is stated in Theorem 2.

Theorem 2. *For all f, if* $\delta G^{(f)} \leq \varepsilon \cdot G_0$ *, the VQD algorithm guarantees a solution that is at least (1-ε) of the optimal value . That is,* $OPT^{VQD} \geq (1-\varepsilon) \cdot OPT$

Proof: Please refer to Appendix A2.

3.3.c Complexity of VQD Algorithm to Solve P1

The complexity of using *VQD* algorithm to solve **P1** is assessed as follows: First, $O(VL)$ is needed to find out all $\eta_{v,l}$,. ***Steps*** 1 and 2 take $O(VL \cdot logVL)$ operations for sorted scheduling. ***Step*** 3 may have $O(VL)$ as the highest amount of operations. After this stage, the worst case for ***Step***s 4 and 5 is $O(V \cdot logV)$ and $O(V^2)$ respectively. Since in general, $V >> L$, the overall complexity is MAX$\{O(VL), O(VL \cdot logVL), O(VL), O(V \cdot logV), O(V^2)\} = O(V^2)$. Considering that **P1** needs to be solved only once every few seconds, it is reasonable to assume that *VQD* can solve **P1** in real time.

3.4 **Real-Time Scheduling and Resource Allocation**

3.4.a Frame-by-Frame Packet Scheduling Algorithm

Once long term bit rate assignment problem is solved, each CS will upload video stream according to the assigned bit rate. However, due to frame-by-frame variations of CQI, it is necessary to solve the real time OFDMA slot assignment problem **P2**. As discussed earlier, **P2** involves three tasks: (a) decide the scheduling priority for each CS; (b) allocate time critical packets to meet real time constraints; and (c) allocate less-critical packets to meet the target bit rate for each video.

For task (a), a utility-based priority function is proposed in this work to assign scheduling priority for each CS in an OFDMA frame. This priority function is based on the unit utility gain, average throughput of individual CSs, and the queuing delay. Specifically, the priority function defined is

$$\phi_v^k(t) = \begin{cases} \frac{U_{v,norm}}{s_{v,k}} \frac{1}{F_v} \frac{1}{C^{\max}} & \text{, if } F_v^{delay}(t) \geq 1 \text{ and } b_{v,k}(t) \neq 0 \\ 1 & \text{, if } F_v^{delay}(t) < 1 \text{ and } b_{v,k}(t) \neq 0, \\ 0 & \text{, otherwise,} \end{cases} \tag{3.13}$$

where

$$U_{v,norm} = \sum_{l=1}^{L} (w_v \cdot u_{v,l}) \cdot a_{v,l} \Big/ U \ ,$$

$$F_v(t) = F_v^{delay}(t) \cdot F_v^{rate}(t) \ , \tag{3.14}$$

$$F_v^{delay}(t) = (D_{v,\max} - \tau_v(t)) \Big/ \Gamma_s \ , \tag{3.15}$$

$$F_v^{rate}(t) = \overline{r}_v(t-1) \Big/ R_{v,\min} \ . \tag{3.16}$$

Note that ϕ_v^k is the priority of the v^{th} CS on SCH k; $U_{v,norm}$ is the v^{th} utility normalized by U in (3.5); $s_{v,k} = \lceil R_v / C_{v,k} \rceil$ is the estimated slots consumption when CQI is $b_{v,k}$; F_v^{delay} is the delay factor [3] with $D_{v,max}$ and τ_v(t); and Γ_s is the guard time and usually is the same as the scheduling period. When $F_v^{delay}<1$, it implies that the queue in the v^{th} CS has the critical packet and should be served at time t. Thus, the ϕ_v^k is assigned with the highest priority. This mechanism is critical for reducing packet loss and maintaining satisfactory utility.

F_v^{rate} is the ratio of the average upload bit rate to the minimum throughput required to maintain utility. The average bit rate of the v^{th} video is evaluated by

$$\overline{r}_v(t) = (1-\rho) \cdot \overline{r}_v(t-1) + \rho \cdot r_v(t), \tag{3.17}$$

where ρ is set as 1/50 for real-time application [21][22]. When $F_v^{rate}<1$, ϕ_v^k should be increased to make up the deficiency. C^{max} is the highest MCS in Table 2.1 and is used to normalize the ϕ_v value within (0, 1).

The steps for frame-by-frame scheduling are as follows:

1. For each CS, assess $\{\varphi'_s\}$ for all the K SCHs by (3.13):

$$\Phi_v = \{k_1, k_2, ..., k_K : \phi_v^{k_1} \geq ... \geq \phi_v^{k_K}\}; \quad v = 1, ..., V, \tag{3.18}$$

where $\varphi_{v,k}$ will be deleted from the Φ_v if there is no more slots available for upload in the k^{th} SCH.

2. Set the priority P_v as

$$P_v = \max\{\Phi_v\}; \quad v = 1, 2, ...V \ . \tag{3.19}$$

3. The CS with the maximum P_v will be scheduled first and allocated to the available SCH k^{sch}, where

$$(v^{sch}, k^{sch}) = \arg\max_{(v,k)}\{P_v\}; \tag{3.20}$$

The instant CQI assigned to v^{sch} at frame t can be shown as

$$b_{v^{sch}}(t) = b_{v^{sch},k^{sch}}(t) \ .$$

This assigned CQI can be mapped to the corresponding MCS m, as shown in Table 2.1, and the MCS adopted by CS v^{sch} is thus obtained. The average CQI is then updated by (3.2).

In our system, we iteratively schedule the CS and select the allocated SCH along with the corresponding MCS using Steps 1, 2, and 3 above for every OFDMA frame until no more slots are available or all payloads have been allocated.

Intuitively, to obtain the optimal utility, the CSs with higher unit utility gain should have higher priority to be scheduled. However, scheduling decisions relying on utility gain only are insufficient to support real time video service due to its strict delay and throughput constraints as well as instantaneous variations in compressed videos. Hence, the F_v factor is included in the proposed function (3.13), where once critical packets exist in a CS, the priority of this CS is raised to the highest value for timely transmission.

However, such an arrangement may lead to a critical question: For CSs with no critical packets, will the policy articulated by (3.13) favor CSs with high utility or good instant CQI and become highly unfair?

To answer this question, we offer the following analysis. Without loss of generality, let us assume the best SCH is used and both $F_v^{delay}>1$ and $b_v>0$ are held for each CS. We also denote $s_v = R_v/C_v$ for brevity of notations. From Eqs. (3.13), (3.15), and (3.16), one has

$$\begin{aligned}\phi_v(t) &= \frac{U_{v,\,norm}}{s_v}\frac{1}{F_v^{rate}}\frac{1}{F_v^{delay}}\frac{1}{C^{\max}} \\ &= \frac{U_{v,\,norm}}{s_v}\frac{R_{v,\min}}{\bar{r}_v(t-1)}\frac{1}{F_v^{delay}}\frac{1}{C^{\max}}.\end{aligned}$$

The average bit rate $\overline{r}_v(t-1)$ in (3,16) can be derived as $C_v^{avg} \cdot S_v^{avg}$, where C_v^{avg} and S_v^{avg} are average slot capacity and average slot assigned respectively. Then the priority function above becomes

$$\phi_v(t) = \frac{U_{v,\,norm}}{R_v/C_v}\frac{R_{v,\min}}{C_v^{avg}S_v^{avg}}\frac{1}{F_v^{delay}}\frac{1}{C^{\max}} = \frac{U_{v,\,norm}}{S_v^{avg}}\frac{C_v}{C_v^{avg}}\frac{R_{v,\min}}{R_v}\frac{1}{F_v^{delay}}\frac{1}{C^{\max}} \qquad (3.21)$$

In (3.21), the C_v/C_v^{avg} indicates that the BS tends to schedule a CS when its instantaneous CQI is high enough relative to its own average CQI over a specific time scale. In short, a CS is allowed to upload data when its CQI is near its own peak. This concept is consistent with the *proportional fair* or *opportunistic scheduling* in [8] and thus (3.21) shows that fairness is in fact already embedded in the proposed algorithm of (3.13). In addition, the spectrum usage efficiency is also sustained by using (3.13) since multiuser diversity can still be benefitted by using proportional fair scheduling, as shown in [8].

The complexity for scheduling by *VQD* priority function in (3.13) is assessed as follows: In (3.18), for each CS, the priority in (3.13) needs to be evaluated for all *K* channels and these *K* results in turn need to be sorted. Thus (3.18) has $O(VK)$ + $O(VK \cdot logVK)$ operations. In regard to (3.19) and (3.20), both require $O(V)$ operations. So the complexity for scheduling is MAX{$O(VK)$, $O(VK \cdot logVK)$, $O(V)$}= $O(VK \cdot logVK)$, which is polynomial time. It is hence justifiable to apply the proposed algorithm to real-time application.

3.4.b Real-Time Slots Assignment

When a CS is scheduled based on its priority, the number of slots allocated to this CS also needs to be decided. The allocated bandwidth must satisfy the $r_{c,v}(t)$ constraint in (3.9) to minimize the cost function *E(t)* defined in (3.10). Besides, for live video, the required rate $R_{v,min}$ must be guaranteed while assigning the UL rate of $r_{c,v}(t)$ and less-critical bits in case the videos become useless due to insufficient bandwidth [31].

Thus, [5][6][11] proposed that the average assigned bit rate at time *t*, as shown in (3.17), should fulfill the condition

$$\overline{r}_v(t) \geq R_{v,\min} \ . \tag{3.22}$$

In [5][6], the amount of bits to be uploaded by each CS is evaluated every OFDMA frame. When the average rate before frame *t*, i.e., $\overline{r}_v(t-1)$, is smaller than $R_{v,min}$, the bits to be uploaded should be increased and assured to satisfy the $R_{v,min}$. Otherwise, no resource is needed. It can be expressed as

$$\Delta_v(t) = \begin{cases} (R_{v,\min} - \overline{r}_v(t-1)) \cdot t_c + \overline{r}_v(t-1), & \text{if } \overline{r}_v(t-1) < R_{v,\min} \\ 0, & \textit{otherwise} \end{cases}, \tag{3.23}$$

where $\Delta_v(t)$ is the rate required to assure $R_{v,min}$, and $t_c = 1/\rho$.

However, the instantaneous channel condition of a mobile client is time-varying and a CS may temporarily suffer from unexpected serious channel fading. In case of slow stations, with high scheduling priority, transmit too many packets through the poor quality channels in order to meet the $R_{v,min}$ requirements, they will definitely consume

even more resource than fast stations do due to poor CQI and the low-efficiency MCS. Under this circumstance, the resource usage efficiency is decreased and other CSs will suffer from resource shortage because of the slot exhaustion caused by slow stations. Thus, the performance of each UL CS and the system throughput are all negatively affected or sacrificed. To overcome this issue, we propose the resource allocation algorithm, shown in Figure 3.3, by modifying (3.23) as follows.

Two situations are considered in our method: (i) when the instantaneous uplink CQI b_v(t) measured by the BS [24] is lower than the average CQI b_v^{avg}, or (ii) the $b_v(t) \geq b_v^{avg}$ but $\overline{r_v}(t-1) \geq R_{v,min}$, then the G_v, derived from (3.3), is imposed as the upper bound for the amount of slots to be assigned to each (say, the v^{th}) CS in each frame. Otherwise, if the b_v(t) is higher than the average, the number of bits allowed for the v^{th} CS's transmission should be assured to satisfy the $R_{v,min}$. The procedure above can be shown by (C1) listed in Figure 3.3.

By imposing the G_v in situation (i), the system can prevent the scheduled CSs with deep channel fading from severe exhaustion of the available slots during transmission [9]. For (ii), even though the average uploaded rate already satisfies the $R_{v,min}$, the bandwidth G_v can still be allocated to scheduled CSs in view of its ability to efficiently decrease the amount of buffered data and the critical packets.

1: Evaluate for each scheduled v[th] CS

2: if $b_v \geq b_v^{avg}$

3: $\Delta_v(t) = \begin{cases} (R_{v,\min} - \bar{r}_v(t-1)) \cdot t_c + \bar{r}_v(t-1), & \text{if } \bar{r}_v(t-1) < R_{v,\min} \\ G_v \cdot b_v(t) \cdot scr, & \text{if } \bar{r}_v(t-1) \geq R_{v,\min} \end{cases}$ (C 1)

4: else

5: $\Delta_v(t) = G_v \cdot b_v(t) \cdot scr$

6: end if

7: Compare $\Delta_v(t)$ and $r_{v,c}(t)$, choose the max. as the bits assigned:

8: $r_v(t) = \max(\Delta_v(t), r_{v,c}(t))$, and thus $S_v(t) = \lceil r_v(t) / (scr \times b_v(t)) \rceil$

Figure 3.3: Pseudo code for proposed resource allocation method.

After $\Delta_v(t)$ is found, we should assure constraint in (3.9) is guaranteed. Thus, the $r_v(t)$ is determined by

$$r_v(t) = \max(\Delta_v(t), r_{v,c}(t)), \tag{3.24}$$

and the number of slots assigned at time t ($S_v(t)$) is

$$S_v(t) = \lceil r_v(t) / (scr \times b_v(t)) \rceil. \tag{3.25}$$

If the available slots on SCH k^{sch} in (3.20) is not enough, the second best SCH for the CS v^{sch} is selected and the remaining bits are allocated [6]. The details for real-time slot assignment are summarized in Figure 3.3.

3.5 Simulation and Performance Comparison

3.5.a Utility-Driven Greedy Algorithm

The performance of the proposed *VQD* algorithm is evaluated through extensive simulations using realistic wireless channel models. Specifically, for bit rate assignment in **P1**, *VQD* will be compared to a baseline Utility-Driven Greedy algorithm over various scenarios [16]-[18].

The baseline Greedy algorithm is initialized by assigning equal amount of resource G_v to each UL CS. The utility U_v and rate R_v of each CS are thus obtained based on G_v and its average CQI, as shown in (3.4).Then the Greedy algorithm iteratively takes away a small amount of assigned slots ΔG from the CS identified to be least sensitive to the utility decrease due to this slots reduction, and then continuously assigns this ΔG to the other CS that can generate the highest utility benefit until no improvement is obtainable.

Let ΔU_v denote the change of utility for the v^{th} CS due to a change of slot ΔG. This algorithm can be expressed as an iterative maximization of the incremental utility by adding ΔG of CS n^+ and decreasing ΔG from CS n^-, such that:

$$n^+ = \arg\max_v (\Delta U_v \,|\, G_v \leftarrow G_v + \Delta G),$$

$$n^- = \arg\min_v (\Delta U_v \,|\, G_v \leftarrow G_v - \Delta G).$$

After the rate R_v is assigned, two well-known schedulers, M-LWDF and EXP [10]-[12], along with the slot assignment strategy in (3.23), are incorporated with Utility Greedy to facilitate live video packet scheduling in **P2**. M-LWDF and EXP are adopted

because of their great QoS performances for real-time flows in cellular systems [10][30], where the former performs well for systems with lower loads, and the latter is recommended for those with higher loads [30].

3.5.b Simulation Configuration and Channel Model

In this paper, the simulations are performed strictly according to [20][27]. The simulated WCN includes one UL BS in the center of cell, and the connected UL CSs are all mobile and uniformly distributed within the cell. To simulate each mobile CS's CQI, the channel propagation loss is estimated based on the COST 231 sub-urban model, and the small scale fading effect is measured employing the ITU Veh-A multipath model [27] corresponding to 30 Km/hour. The simulation (I) and (II) below are set to work on a 5 MHz and 10 MHz bandwidth with a 5ms OFDMA frame [27] respectively, and both adopt the band-AMC permutation [20] for sub-channelization. Table 3.2 summarizes the system parameters used in the simulation, and the parameters of OFDMA band-AMC mode are shown in Table 3.3.

Table 3.2: System Parameters

Parameters	Value
Operating frequency	2.5 GHz
Duplex	TDD
Channel bandwidth	10 MHz
Cell radius	1.4 km
BS Height	32 m
MS Height	1.5 m
BS Antenna Gain	15 dbi
MS Antenna Gain	-1 dbi
Antenna Pattern	70° (-3 dB) with 20 dB front-to-back ratio
MS Noise Figure	7 dB

Table 3.3: Band-AMC OFDMA Parameters

Parameters	Value
Permutation mode	Band-AMC
FFT size	1024
Sub-carrier frequency spacing (f)	10.94 kHz
Useful Symbol Time ($T_b = 1/f$)	91.4μs
Guard time ($T_g = T_b /8$)	11.4 μs
OFDMA Symbol Duration ($T_g = T_b + T_g$)	102.9 μs
Frame duration (t_{fr})	5 ms
Number of OFDMA Symbols	48
Band-AMC Mode	
Null sub-carriers	160
Pilot sub-carriers	96
Data sub-carriers	768
Number of Sub-carrier per slot	48

3.5.c Simulation (I): Packet Scheduler Performance

In the first simulation, we only compare the performance of different packet schedulers, including *VQD*, and the M-LWDF and EXP in Sec. 3.5-(A). We assume that 6 CSs are uniformly scattered in a WCN, which is a 5-MHz OFDMA system. Each CS has a constant bit rate (CBR) video with 1 Mbps. Without loss of generality, we use the

Table 3.4: The average Throughput (Kbps).

	G_0=198	G_0=176	G_0=154
VQD	6124.98	6119.01	6043.39
M-LWDF	5968.90	5928.75	5847.11
EXP	5965.30	5930.91	5850.86

Table 3.5: The average packet loss (%).

	G_0=198	G_0=176	G_0=154
VQD	0.3	0.34	1.57
M-LWDF	2.58	3.37	4.77
EXP	2.66	3.31	4.63

normalized utility, i.e., $u_{v,l}$ =1, since only one rate mode is used. To ensure real-time streaming, the $D_{v,\max}$ = 50 ms for each packet [9][37]. Besides, three resource scenarios (176, 154, and 198 slots for UL) are used for comparison. In the first scenario, 176 slots can be considered as 50% of total slots in a 5MHz OFDMA frame and is abundant for all 6 CBR videos being uploaded if the resource is efficiently assigned. The other two scenarios, with lower and higher resource budgets, are also tested for more comparisons. The experimental results are summarized in Table 3.2 and 3.3. It is evident that by jointly considering the factors in (3.14), the concept of opportunistic scheduling, and the slot assignment method in Figure 3.3, the *VQD* packet scheduler can not only effectively enhance the throughput but also greatly decrease the system packet loss, even the available slot budget is tight.

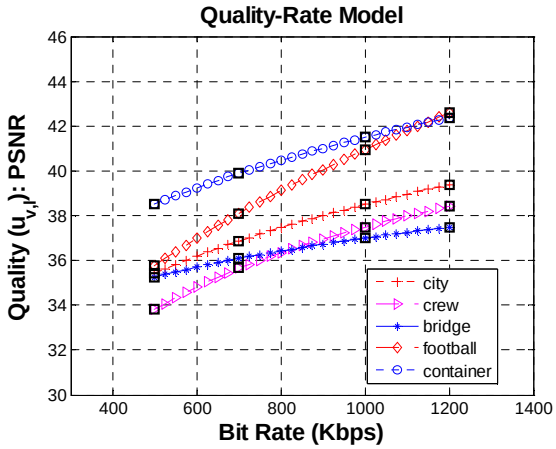

Figure 3.4: Quality ($u_{v,l}$) – Rate models for the 5 videos used in simulation. The "□" denotes the quality of each $R_{0,l}$. [29][35]

3.5.d Simulation (II): Systematic Method Performance

In this simulation, a WCN with 20 uniformly distributed UL mobile CSs is considered. Each CS is assigned to a weight integer w_v within the range from 1 to 3, and provided a live video which is encoded by H.264/AVC with L = 4 allowable target bit rate modes, i.e., $\mathbf{R}_0$=[$R_{v,l}$]=[500, 700, 1000, 1200] Kbps. The PSNR, an objective quality measurement, is adopted to assess the video quality ($u_{v,l}$) at different bit rates in our simulation. Figure 3.4 shows the quality-rate functions for 5 different videos encoded with the H.264 AVC codec at CIF resolution and a frame rate of 30 frames/sec [29][35]. Each CS is randomly assigned to one of the compressed video streams (with different quality-rate model) to be uploaded to the BS, then the video quality and utility to be uploaded to the BS can be evaluated by these models based on the target bit rate, as the works in [16]-[18][33]. Again, to ensure real time video streaming, the $D_{v,\max}$ = 50 ms is used.

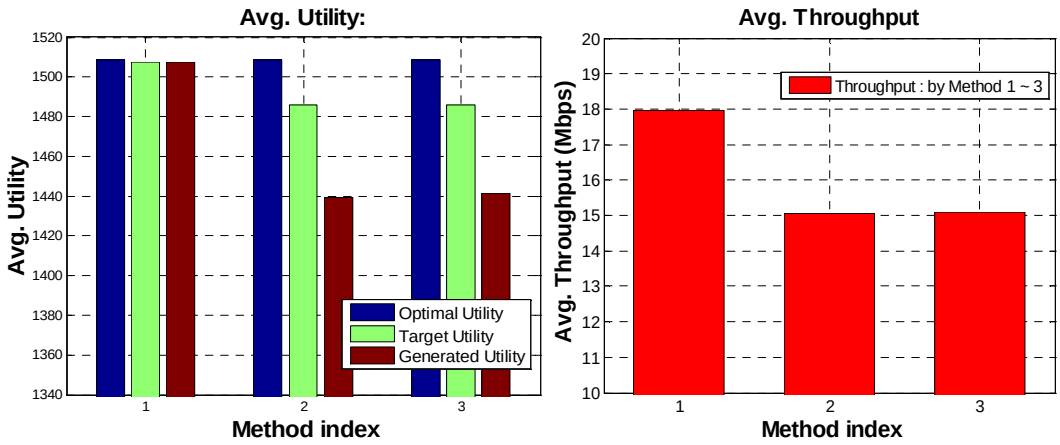

Figure 3.5: Comparisons of different Methods, 1: *VQD*, 2: Utility Greedy with M- LWDF, 3: Utility Greedy with EXP: (a) avg. utility: Optimum vs Target vs Generated in 30 secs, and (b) Avg. throughputs in 30 secs.

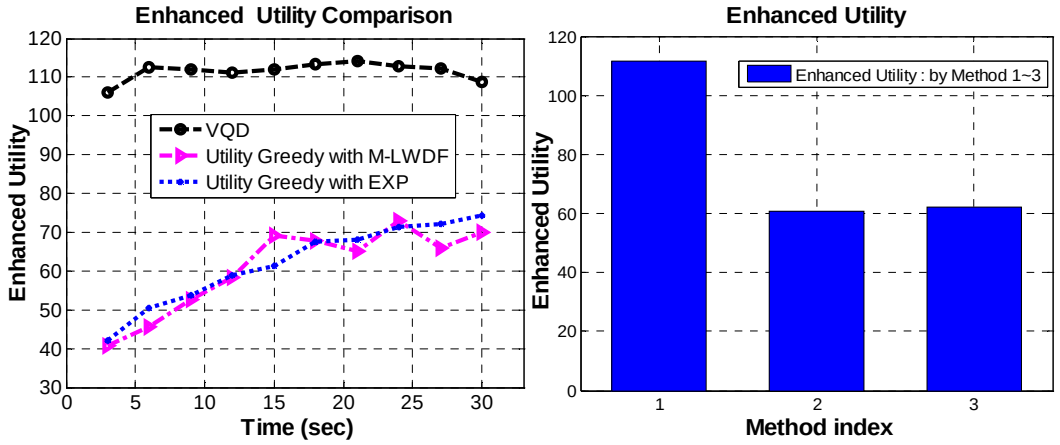

Figure 3.6: (a) System enhanced utility every 3 secs. (b) Enhanced utility in 30 secs by method 1: *VQD*, 2: Utility Greedy with M-LWDF, 3: Utility Greedy with EXP.

Four UL systematic algorithms are compared: 1) the proposed *VQD* method, 2) the Utility-driven Greedy method incorporated with M-LWDF, and 3) the Utility-driven Greedy method with EXP scheduler, and 4) the globally optimal utility by Exhaustive

search. Each method needs to solve **P1** to decide the R_v and target utility for each CS, and then real time schedulers adopted in 1), 2) and 3) have to solve **P2** to find the utility actually being generated. As for 4), we assume the target R_v and utility can be perfectly reached to the optimum and thus no scheduler is needed to solve **P2**. The utility produced by each CS is updated every 3 seconds. The total slots per frame reserved for UL video (G_0) is 495.

The overall system performance are summarized in Figs. 3.5 ~ 3.7. Figure 3.5(a) shows the average utility comparisons in 30 secs and both the target and generated utility by *VQD* being much closer to the optimum by 4) than those by the other methods. Figure 3.5(b) indicates that the throughput by *VQD* is clearly higher than those by 2) and 3), suggesting the much improved spectrum usage efficiency by *VQD*.

Furthermore, for each method, the G_0 in the simulation is in fact allowing all CSs to upload videos by using a basic bit rate of 500 Kbps to generate the basic utility. Therefore, the real meaningful aspect here is to compare the enhanced utility, i.e., the increased utility obtained by each method above the basic utility portion. Figure 3.6(a) shows that the enhanced utility produced by *VQD* is consistently far better at each moment, and Fig. 3.6(b) exhibits the enhanced utility by *VQD* is some 80% higher on average than those obtained by other methods.

Figure 3.7 shows system loss rate by proposed *VQD* packet scheduler and Utility Greedy with different schedulers. The *VQD* packet scheduler maintains better performance because it assigns the highest priority to the CS with time critical packets,

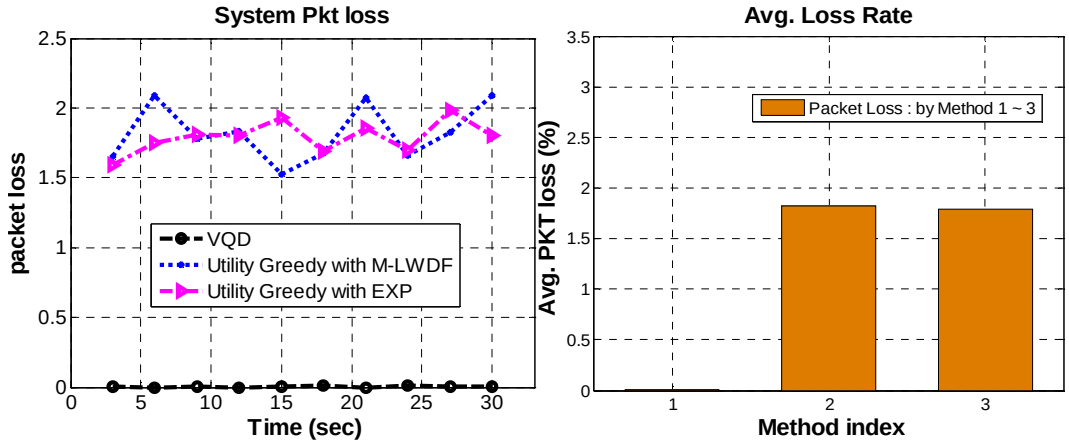

Figure 3.7: (a) System packet loss every 3 secs. (b) Packet loss in 30 secs by 1: *VQD*, 2: Utility Greedy with M-LWDF, 3: Utility Greedy with EXP.

consequently providing better QoS than the others, as has been covered in [4]. According to [30], the M-LWDF provides better QoS to systems with lower loads, and the EXP is recommended for those with higher loads. Since the Utility Greedy assigns the bit rate based on the available slots and the capacity of each CS, the UL traffic is basically appropriately allocated and thus the results for method 2 and 3 are similar.

In addition, the utility Greedy method needs to search the most appropriate CS pairs to exchange the assigned resource for the optimal utility. This task becomes more complicated due to the fluctuating or changing channel qualities of mobile CSs. Since the best CS pairs and the slots exchanged may not be that easy to obtain, it thus takes longer execution time to find the optimum, as can be seen in Fig.3.6. *VQD* simply assigns resource according to the $\eta_{v,l}$ in (3.12), and then enhances the results by applying ***Steps*** 3 to 5 in Sec. 3.3.(a) when needed. Using this simpler procedure, the *VQD* can quickly find the near-optimal solution and can be easily implemented in the wireless UL scenario.

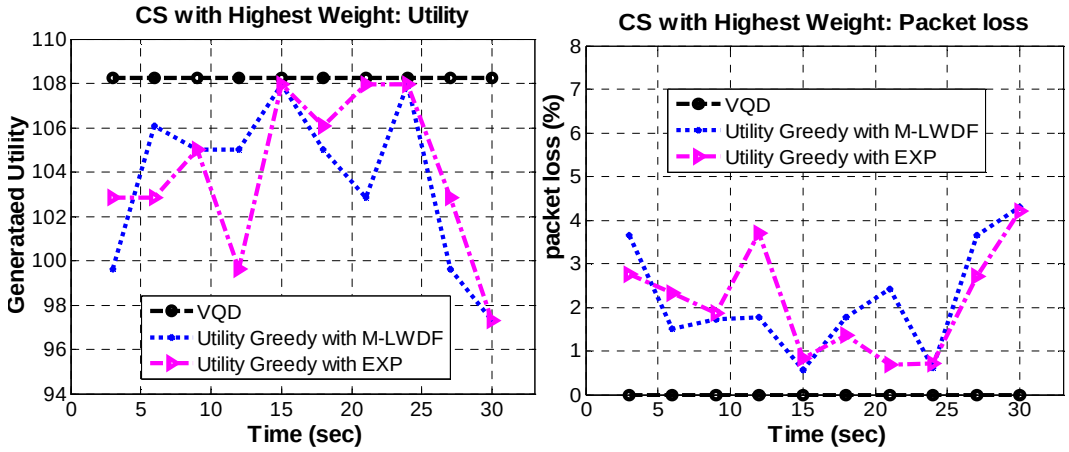

Figure 3.8: (a) Utility and (b) Packet loss every 3 secs. A CS with highest weight is randomly selected.

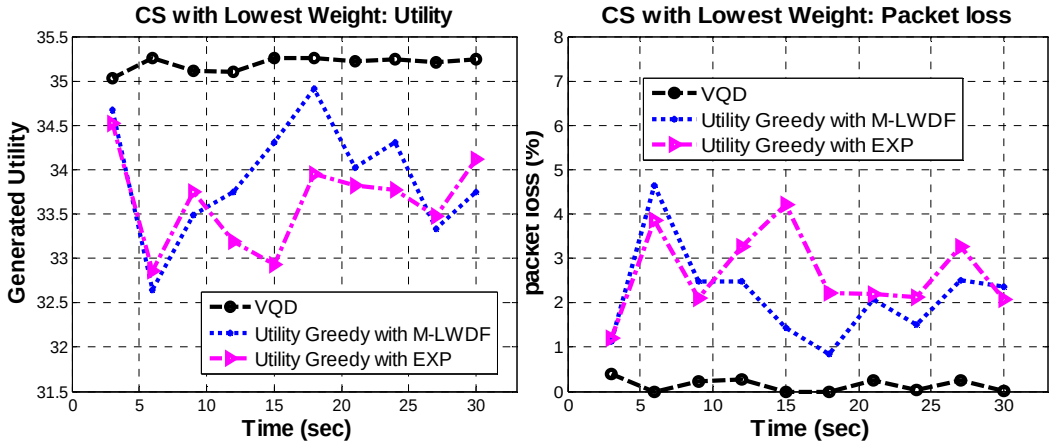

Figure 3.9: (a) Utility and (b) Packet loss every 3 secs. A CS with lowest weight is randomly selected.

Figures 3.8 and 3.9 show the performances of the videos randomly selected from the highest and the lowest weighted CSs respectively. Compared with the other methods, the *VQD* provides higher and more stable utility and lower packet loss for all videos. Figures 3.8(b) and 3.9(b) implies that the *VQD* scheduler further guarantees the low loss of important videos.

Chapter 4 –Resource Allocation for Integrated Real-Time Scalable Video System over OFDMA Mobile Network

4.1 Overview for Integrated Real-Time Video System

Thanks to the success of wireless broadband access technologies, the mobile real-time video uplink application, which integrates wireless camera or ad-hoc wireless video sensor networks with mobile/portable devices, is nowadays feasible[1][2]. With such a system, video cameras/sensors are mounted on mobile devices, such as mobile phones or vehicles, to capture videos of particular targets or live events and immediately upload the captured videos via wireless channels to a centralized repository or social web platforms having capability to deliver live videos, such as YouTube [73], Twitter, Facebook, etc, for real-time sharing, distributing, and recording.

In our proposed framework, the uploaded videos are not only real-time collected, but also their distributions considered. The live video streams, once available, are announced or pushed to the users subscribing to the channels on web platforms. The users linking to the channels to receive the videos are seen as mobile station (MS) subscribers. Multicasting or broadcasting is adopted to expedite the downlink live video delivery to all the MSs to ensure efficient use of radio resource. A conceptual diagram of this proposed framework is shown in Fig. 4.1.

The key innovation of this proposed framework is the use of perceived quality of DL subscriber to decide how the UL radio resource should be assigned. This end-to-end

optimized approach ensures the most efficient allocation of limited radio resources while strives to achieve the desired performance. In addition, with increasing demands for high data rate video service in wireless networks, the layer-encoded technology, such as scalable video coding (SVC) [49]-[52], which provides spatial, temporal, and quality scalability for video streaming services and achieves flexible data rate adaptation for real-time video delivery, is adopted as the APP layer solution. Moreover, the structure for UL SVC camera is clearly defined. The UL bitstreams of base and enhancement layers in CSs are classified into different queuing buffers, which can be identified by the BS, and one connection session will be initially created for each layer [68]. The BS can thus correctly estimate the utility for each UL layer and more efficiently assign the limited UL resource. Compared with the traditional non-layered video, the SVC can quickly adapts its UL rate with nearly no delay by determining the number of UL layers. Thus, it obviously has faster reaction to variable channel conditions and is certainly a better choice for the real time video system.

In a realistic wireless environment, the radio spectrum is limited and the channel conditions of UL CSs or DL MSs vary frequently over time and space. For efficient video delivery in a WCN, the number of video layers assigned to each UL CS should be determined according to the available radio resource and corresponding utility, i.e., the DL users' perceived video quality in this work. Moreover, the real-time scheduling and MCS selections for all the occupied SCHs at the BS should be carefully chosen for both UL and DL. Based on these settings, a joint UL/DL resource allocation problem is

formulated and solved in this chapter. Specifically, the objective is to maximize the satisfaction of subscribing MSs by effectively scheduling and allocating resource to the UL videos from all CSs. Toward this goal, a visual quality driven resource allocation method, incorporating the DL multicast algorithm, is proposed to quickly and effectively obtain the best target utility and determine the number of video layers to be uploaded for all UL CSs. Further, in order to guarantee the target utility can be reached, a utility-based priority function is designed for real-time packet scheduling. The complexity analysis results indicate that the solution can be achieved in polynomial time.

Further, to maximize the distributing efficiency of the DL videos to all MSs and concurrently optimize their satisfaction, a previously proposed opportunistic layered multicasting (OLM) scheduling algorithm [13] is applied. In our integrated system, the OLM is further adopted to (i) estimate the number of DL MSs to receive a certain video layer in real-time so that this layer's utility can be found immediately, and (ii) select the UL CSs to transmit more layers in order to optimize the system's total utility.

The rest of this chapter is organized as follows. Section 4.2 will first introduce our previously published OLM multicast scheduling algorithm, which has been adopted as the solution of DL side in our proposed integrated framework. The resource management problem of integrated system and the proposed cross-layer solutions are detailed in Section 4.3 and 4.4. The simulation results and discussions will be covered in Section 4.5.

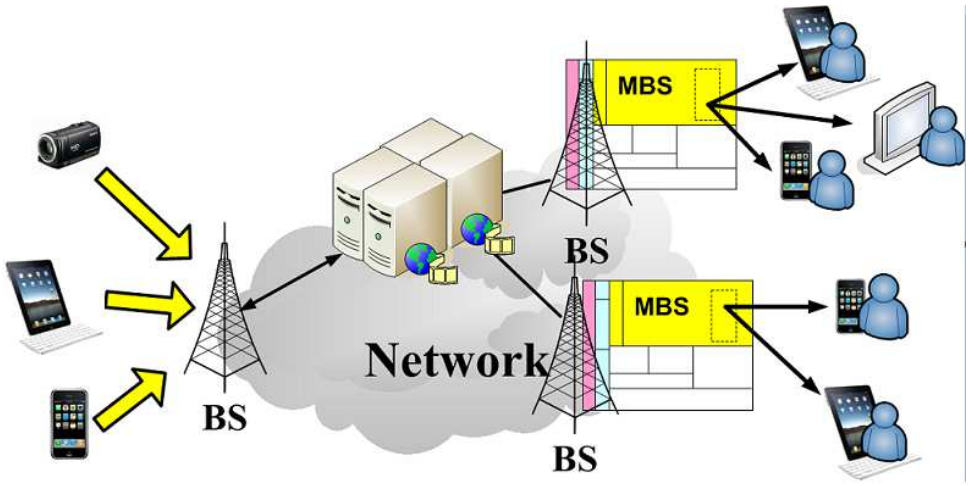

Figure 4.1: The integrated Real-Time video system over OFDMA-based mobile networks: Unicast for UL and multicast for DL

4.2 **Opportunistic Layered Multicasting (OLM) over 4G Network**

As introduced in Sec. 1.1 and 4.1, our integrated system adopts SVC video to facilitate more flexible data rate adaptation and applies the previously proposed OLM algorithm [13] to distribute the videos to MSs. Besides, the OLM is further adopted to (i) estimate the number of DL MSs that can receive a certain video layer whenever the system obtains the MS's CQI feedback so that this layer's utility can be found immediately, and (ii) select the UL CSs to transmit more layers in order to optimize the system's total utility. We thus provide a brief introduction for OLM algorithm in this section.

4.2.a Downlink Resource Management Problem

After each DL BS receives the videos, it has to immediately multicast these live videos to all concerned MSs. However, conventional multicast schedulers intend to serve all the subscribers in each transmission instance by choosing the MCS that has a lower SNR requirement to meet the channel condition of every MS. This results in conservative MCS adoption at the multicast schedulers, and the performance such as system throughput of real-time video multicasting will be bounded by the worst fading channel condition among all the MSs at each transmission instance.

By incorporating multiuser diversity into DL multicast scheduling, OLM algorithm [13] chooses MCS more aggressively, i.e. it may choose higher MCS, at the BS and allows the DL system to ride the peaks of the MSs' fading channel fluctuation. To achieve higher efficiency of selecting MCS, the OLM is also facilitated by block erasure forward error correction (FEC) code [13] [64], such as fountain codes. Thus, the MSs can recover the original video contents as long as they have received enough encoded OFDMA frames.

Furthermore, since the scalable video, consisting of a mandatory (base) layer and optional (enhancement) layers, is adopted in the integrated system, the OLM scheduler needs to select the number of receivers, i.e., the subset of targeted MSs, for each video layer. Once the subset of targeted MSs is determined, the best MCS and FEC parameters to transmit each video layer can also be decided, and the possible utility for each layer can thus be estimated. As a result, after the number of scalable video layers

has been determined and the layers uplinked, the OLM scheduler can efficiently multicast the video streams to MSs based on their CQI feedbacks and hence provide adequate video playback resolution matching MSs' channel quality. The following subsections will further explain our strategies.

4.2.a.(i) Notations and Formulation of Resource Consumption

Before describing our strategies, several notations need to be defined. Assuming there are V DL layered video streams to be multicast in a specific WCN, and the total slots for MBS in an OFDMA frame is limited to G_{DL}. Further, the number of MSs subscribing to the v^{th} video is noted as $N_{v,}$ and the number of MSs that receive the v^{th} video with up to l^{th} layer delivered is noted as $N_{v,l}$, where $v = 1, \ldots, V$ and $l = 1, \ldots, L$. Clearly, $0 \le N_{v,l} \le N_v$.

Now we can formulate resource consumption under opportunistic multicasting scheduling. For each v^{th} video stream, suppose the original data rate of the l^{th} video layer, noted as (v, l), is $\delta R_{v,l}$. Because of using application level FEC, the original video stream (v, l) is expanded from video source data rate $\delta R_{v,l}$ to $\delta D_{v,l}$.at code rate r (to be addressed later). In a SVC system with CBR for individual layers, the average number of slots consumed S^t at the t^{th} OFDMA frame for (v, l) can be evaluated as

$$S^t = \left\lceil \frac{\delta D_{v,l}}{C(m^t)} \right\rceil , \tag{4.1}$$

where the $C(m)$ is the slot capacity when MCS m is decided, as shown in Table 2.1.

The average throughput successfully decoded for user i is subject to the channel quality dependent indicator function and expressed as:

$$\overline{T}_i = \lim_{t\to\infty} \frac{1}{t} \sum_{j=1}^{t} I(m^j, b_i^j) \cdot \delta D_{v,l} \tag{4.2}$$

where $I(m^j, b_i^j)$ is an indicator function that equals 1 if user i can correctly decode transmitted data and 0 otherwise, given current CQI b_i^j and the selected MCS m^j.

From (4.2), we define $\overline{Q}_i$ as average OFDMA frame receiving rate

$$\overline{Q}_i = \lim_{t\to\infty} \frac{1}{t} \sum_{j=1}^{t} I(m^j, b_i^j), \tag{4.3}$$

representing the percentage of frames user i receiving given the MCS set. If the application layer FEC, such as Reed-Solomon codes or Raptor codes, is applied, the ideal code rate to serve all subscribers $N_{v,l}$ is the minimum $\overline{Q}_i$ among them, i.e., $\min_{i\in N_{v,l}} \overline{Q}_i$. This derived amount of FEC can support data rate at $\min_{i\in N_{v,l}} \overline{T}_i$ to be correctly decoded with high probability [64].

Thus, in order to deliver a video layer, the system requires to spend resource at least maintaining $\min_{i\in N_{v,l}} \overline{Q}_i \cdot \delta D_{v,l} = \delta R_{v,l}$ to serve a user set $N_{v,l}$. The average number of slots (amount of resource) in a frame consumed by this layer for an admitted user set can be further formulated by substitute $\delta D_{v,l}$ in (4.1) by using the aforementioned criterion :

$$\overline{S}_{v,l} = S(N_{v,l}) = \lim_{t\to\infty} \frac{1}{t} \sum_{j=1}^{t} \left\lceil \frac{\delta R_{v,l}}{C(m^t) \cdot \min_{i\in N_{v,l}} \overline{Q}_i} \right\rceil. \tag{4.4}$$

4.2.a.(ii) Optimization on Mandatory Video Base Layer

The base layer of a video contains the most significant information of that video. Therefore, each MS should receive this layer in OLM for basic service assurance. Based on this guideline, all MSs of the v^{th} video should be included in the subset of target MSs, noted as $\{N_{v,l},\ l=1\}$. This guideline may result in low MCS adopted due to the MS possibly having the worst channel condition. Nevertheless, to optimize the total utility, we should try to decrease the resource consumed by base layer so that more enhancement layers can be transmitted.

As a result, in the first optimization problem, the objective is to efficiently (i.e., using least amount resource units) multicast the base layer (l=1) with basic perceptual quality, to all subscribers. Note that, in this scenario $N_{v,1} = N_v$. The amount of resource consumed in (4.4) can be minimized when we maximize the minimum effective throughput across all users by dynamically adapting MCS of allocated slots

$$\begin{aligned} \widetilde{m} &= \arg\min_{m} S(N_v) \\ &= \arg\max_{m} \left\{ C(m) \cdot \min_{i \in N_{v,l}} \overline{Q}_i \right\} \end{aligned} \tag{4.5}$$

subject to $$\sum_{v} S_{v,1} \le G_{DL}$$

Only the base layers associated with all the videos channels are considered in case when the required number of slots are more than total preallocated number of slots U for the video multicasting service. In this case, to ensure all base layers are allocated,

subscribers with worst channel quality can be dropped from N_v to allow the choices of more efficient MCS indices so that the total resource budget can be within G_{DL} slots.

4.2.a.(iii) Optimization on Optional Video Enhancement Layers

The enhancement layers of a video contain optional information of that video, so their priorities of resource allocation are lower than that of the base layer.

After the optimization is carried out for multicasting of base layers, the remaining resources are used to allocate optional video enhancement layers, from which only a subset of users are scheduled to receive, subject to the maximization of a system-wide transmission gain constrained by available resources. The transmission gain used in our formulation is represented by utility functions, $\delta u_{v,l}$, corresponding to subjective video quality gain of user experiences when the l^{th} enhancement layer of the v^{th} video is successfully received and decoded subject to layer dependency, i.e., a scheduled user is allowed to subscribe the l^{th} video layer only if all the lower layers are also subscribed. In consequences, the optimization problem jointly considers scheduling (i.e., determine video layers to transmit to a subset of scheduled users) and the resource allocation (i.e., adapting MCS) can thus be formulated as

$$\max \sum_{v=1}^{V} \sum_{l=1}^{L} \delta u_{v,l} \cdot N_{v,l} \tag{4.6}$$

subject to $$\sum_{v} S_{v,1} \leq G_{DL}$$

where $0 \leq N_{v,l} \leq N_v$. We maximize the total utility gained by all scheduled users given the resource constraint and inherited nature of layer dependency.

Equation (4.6) requires that a good scheduling candidate should provide maximum utility gain per unit of resource. In other words, to accomplish (4.6), it is equivalent to solving the subproblem of maximizing the unit utility gain of a specific pair of (v, l), by searching the best MCS $\widetilde{m}$ and the best set for users $\widetilde{N}_{v,l}$.

$$\begin{aligned}(\widetilde{m}, \widetilde{N}_{v,l}) &= \arg\max_{(m,N_{v,l})} \frac{\delta u_{v,l} \cdot N_{v,l}}{\overline{S}_{v,l}} \\ &= \arg\max_{(m,N_{v,l})} \left\{ C(m) \cdot \min_{i \in N_{v,l}} \overline{Q}_i \right\} \cdot N_{v,l},\end{aligned} \tag{4.7}$$

The eq. (4.7) can be derived because the $\delta u_{v,l}$ and $\delta R_{v,l}$ in (4.4) are constant given a specific (v, l).

In the following subsections of *4.2.b ~ 4.2.d*, we detail the algorithms designed to solve the corresponding optimization problems, as shown in (4.6) and (4.7), with OFDMA-based specification in mind. Different strategies are conducted to base and enhancement layers. Besides, FEC is implemented in a cross-OFDMA-frame fashion and finite block size N, i.e., every N OFDMA frames.

4.2.b Adaptive FEC Code Rate Determination

To ensure every subscriber in $N_{v,l}$ can receive the video data while choosing the higher rate MCS, we propose a dynamically adjustable flow-based block erasure (N, K^e) FEC scheme to protect the multicast data, where the e^{th} FEC block uses K^e frames to carry the original data and N-K^e frames to carry FEC redundancy. In other words, the e^{th}

FEC block contains N frames from frame (e-1)N+1 to frame eN, and if a MS can successfully decode the data blocks from at least K^e frames out of the N frames in the e^{th} FEC block, it can fully recover the original data carried in the e^{th} FEC block. We choose to adapt K^e with a predefined length N when generating FEC code to bound the maximum FEC latency. More specifically, we use a system with 5ms OFDMA frame and N = 200, this results in one second of delay. The resource efficient value of K^e is determined by

$$K^e = \begin{cases} \lfloor N \cdot \min_{i \in N_{v,l}} Q_i^{(e-1)N} \cdot f_m \rfloor, & b > 1 \\ \lfloor N/2 \rfloor, & b = 1 \end{cases} \tag{4.8}$$

The average frame receiving rate Q_i^t, instead of using (4.3), is updated by exponentially weighted recursion for real-time scheduling

$$Q_i^t = \begin{cases} (1-\frac{1}{t_c})Q_i^{t-1} + \frac{1}{t_c} I(m^{t-1}, b_i^{t-1}), & \text{t} > 1 \\ 1, & \text{t} = 1 \end{cases} \tag{4.9}$$

where t_c is the window size; f_m is an error margin factor which can statistically guarantee the performance. More detailed discussions for the setup of f_m can be seen in [13].

For implementation, a BS applies fragmentation/aggregation on the video bit streams to from N equal data blocks given the FEC parameter (N, K^e) at overall data rate $\delta R_{v,l} \cdot (N/K^e)$, i.e., $\delta R_{v,l} / K$ per OFDMA frame. The data block defines the amount of data to be allocated in each OFDMA frame, which must allocate sufficient number of slots for it. Thus, the code rate of the e^{th} FEC block, noted as r^e, is

$$r^e = \frac{K^e}{N}$$

4.2.c Mandatory Video Base Layer Allocation

To effectively implement the optimization problem of (4.5), the designed algorithm searches for the best MCS every OFDMA frame to heuristically approach $\max\{C(\tilde{m}) \cdot \min_{i \in N_{v,l}} \overline{Q}_i\}$ series as well as the least resource consumption. The MCS is decided by maximizing the new contributor to the series as

$$\tilde{m}^t = \arg\max_{m \in M} \left\{ C(m) \cdot I(m, b_{\tilde{i}}^{t-1}) : \tilde{i} = \arg\min_{i \in N_v} Q_i^t \right\} \quad (4.10)$$

We jointly consider the maximization of $C(\tilde{m})$ and $\min \overline{Q}_i$ by greedily selecting the MCS $\tilde{m}^t$ for the t^{th} frame based on (4.10). Specifically, according to the most updated CQI feedback, the BS identifies the subscriber $\tilde{i}$ with minimum Q_i^t and then selects the best MCS that the subscriber $\tilde{i}$ can decode.

Besides, at the end of an FEC block, its code rate r^b is updated to ensure efficient usage of resources and keeps up with possible channel quality fluctuation. The procedure for base layer allocation is shown in Figure 4.2. The complexity of the overall loop is O(N_v).

1: $e=1;\ t=1;\ K^e=\lfloor N/2 \rfloor;\ Q_i^t=1\ ;\ \forall i \in N_v$

2: **repeat** $b_v \geq b_v^{avg}$

3: update channel quality b_i^{t-1} and matrix $I(m^{t-1}, b_i^{t-1})$

4: evaluate Q_i^t using (4.9)

5: find $\tilde{i} = \arg\min_{i \in N_v} Q_i^t$

6: find optimized $\tilde{m}^t = \arg\max_{m \in M} \left\{ C(m) \cdot I(m, b_i^{t-1}) \right\}$

7: schedule $\delta R_{v,l}/r^e$ of data to be delivered in the t^{th} frame's OFDMA MBS region using $\tilde{m}^t$

8: **if** end of the t^{th} FEC block **then**

9: $e = e + 1$

10: update K^e using (4.8)

11: **end if**

12: $t = t + 1$

13: **until** end of video session

Figure 4.2: Pseudo code for mandatory base layer allocation

4.2.d Optional Video Enhancement Layer Allocation

For enhancement layers allocation, we execute the optimization formulation of (4.7) by approaching optimal $\tilde{m}_{v,l}^t$ every OFDMA frame and updating $N_{v,l}$ every FEC block. In other words, within an FEC block, a pair of (*v, l*) is targeted to a fixed set of users, who are dynamically scheduled frame-by-frame within the block. The algorithm in Fig. 4.3 describes the whole process.

In searching for $\tilde{m}_{v,l}^t$, operations in Lines 3 to 6 in Figure 4.2 are executed first to calculate $\tilde{m}_{v,l}^t$ and compute the utility function

1: **repeat**
2: **for** all eligible (*v, l*) **do**
3: find $\tilde{m}_{v,l}^{t}$ using Fig. 4.2, Line 3 to Line 6 $\forall i \in N_{v,l}$
4: calculate $\tilde{\eta}_{v,l}$ using (4.11)
5: **end for**
6: schedule (*v, l*) in descending order of $\tilde{\eta}_{v,l}$ until no resource left subject to layer dependency
7: **if** end of an FEC block **then**
8: **for all** eligible (*v, l*) **do**
9: find $\tilde{i} = \arg\max_{i \in N_v} \left| j : Q_j^t \geq Q_i^t,\ j \in N_v \right| \cdot Q_i^t$
10: update $N_{v,l}$ using the result of Line 9
11: **end for**
12: update K^e using (4.8)
13: **end if**
14: **until** end of video session

Figure 4.3: Pseudo code for optional enhancement layer allocation

$$\tilde{\eta}_{v,l} = \frac{\delta u_{v,l} \cdot N_{v,l}}{\overline{S}_{v,l}} = \delta u_{v,l} \cdot N_{v,l} \cdot \frac{C(\tilde{m}_{v,l}^{t}) \cdot r^{b}}{\delta R_{v,l}} \qquad (4.11)$$

of each (*v, l*) according to (4.7). Therefore, we schedule video layers in a descending order of $\tilde{\eta}_{v,l}$ value until no resource left subject to layer dependency. Note that $N_{v,l}$ and r^e are fixed during this phase.

At the end of an FEC block, in addition to update K^e, the algorithm searches for the best subset of users to receive this layer of video by picking the bottleneck station $\tilde{i}$ resulting maximum utility. So, we consider all *i* dependent terms in (4.11) to find

$$\tilde{i} = \arg\max_{i \in N_v} \left| j : Q_j^t \geq Q_i^t,\ j \in N_v \right| \cdot Q_i^t \qquad (4.12)$$

where resulting $N_{v,l} = \{ j : Q_j^k \geq Q_{\tilde{i}}^k,\ j \in N_v \}$ implies only stations capable of receiving more OFDMA frames than $\tilde{i}$ are scheduled for this layer. So, the best $N_{v,l}$ can be continuously updated. The decoupling of $\tilde{m}_{v,l}^t$ (every frame) and $N_{v,l}$ (end of FEC block) searching results in suboptimal allocation but makes sure that once a station is chosen to be served, the whole FEC block will not be interrupted. Comparing to the base layer algorithm, the extra loop updating $N_{v,l}$ has the same search range N_v, so the complexity is still O(N_v).

4.2.e Performance Evaluation for Multicast Algorithms

In this experiment, we focus on the comparison of different multicast algorithms for layered video over 4G network. Two multicast scheduling frameworks are considered: 1) the OLM algorithm in [13], and 2) conventional multicast scheduling algorithm, which is introduced in [15]. The configurations of the simulated system are set based on the PUSC mode [20][27]. Details of the simulation platform can be found in [13][56] and are omitted here due to the space limitation. The basic configurations of WiMAX PHY layer and MAC layer are identical for both methods. In particular, it is assumed that the WiMAX service will be delivered by a single BS to groups of MSs. These MSs shall randomly scattered over the cell area centered at the BS with a radius of 1.4 km. The channel propagation loss is estimated using the COST 231 suburban model and the Jake's model is adopted for the effect of small scale fading [27].

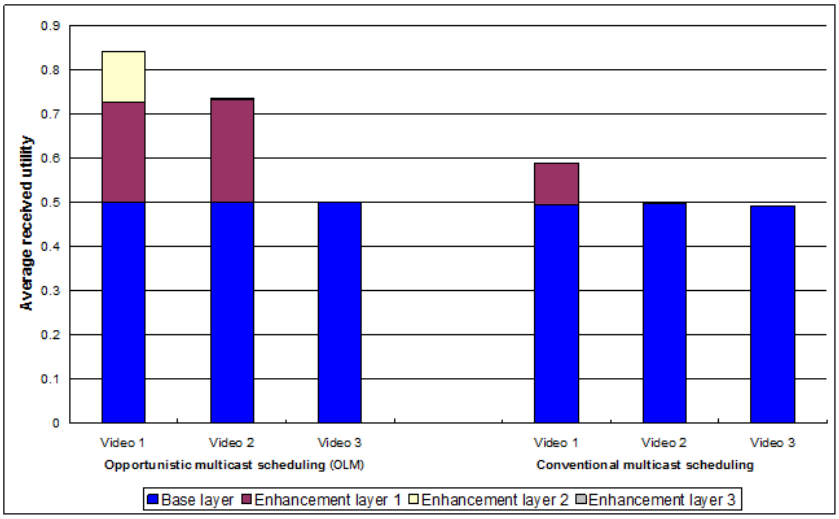

Figure 4.4: Comparison of average received utility

Further, we set up a scenario with three layered video streams ($V = 3$) and the numbers of subscribers are N_v ={100, 80, 40} for three videos respectively. Each DL video has four video layers ($L = 4$), and the utility value for each layer is $\delta u_{v,l}$ = {0.5, 0.25, 0.15, 0.1}. The MBS region size reserved for DL video multicasting is G_{DL}=110 slots. The data rate of each layer is 250 Kbps and will consume an aggregate rate of 1Mbps.

Figure 4.4 shows the average received utility under different algorithms. The OLM can receive 0.74 utility in average from the three videos under the scenario with tight resource budget. Compared with the conventional multicast scheduling which receives only 0.54 utility in average, the OLM achieves 37.9% higher utility, which clearly demonstrates the outstanding performance of OLM algorithm..

4.3 **Resource Management Problem Formulation for Integrated SVC System**

In section 4.2, the OLM multicast scheduling algorithm, i.e., the DL side solution in our proposed integrated framework, has been detailed. In the following sections, we will focus on resource allocation for UL videos by jointly considering the DL MSs.

4.3.a Video Layer Assignment Problem

To tackle the varying wireless channel condition, the layer-encoded video is adopted in our systematic solution. Our UL CSs will directly upload the layered video streams but the number of video layers must first be determined before uploading. Assume V video streams, each captured by a CS, are to be uploaded to the video repository or social web platforms and L is the total number of layers in each video. The rate of the l^{th} layer in the v^{th} SVC video is specified by $\delta R_{v,l}$ in bits/sec (bps), where l = 1 for base layer, l = 2 for first enhancement layer and so on. Besides, for SVC videos, if the l^{th} layer is to be uploaded, it implies that all its lower layers, i.e., l =1, … , (l -1), are already uploaded because of the dependency among layers of SVC coded videos. Thus, for the v^{th} video, when the l^{th} layer is assigned, the overall encoding rate is described as

$$R_{v,l} = \sum_{l''=1}^{l} \delta R_{v,l''}$$

More specifically, we denote $\mathbf{R}_0=[\delta R_{v,l}]$ (in bps) to be an $L \times 1$ vector consisting of the bit rates of each layer, e.g., $\mathbf{R}_0$= [250 250 250 250]^T Kbps, $l=1,\ldots,4$, and each CS needs to be

assigned the number of uploaded layers so that the target bit rate can be determined. Further, we define a $1 \times L$ *assignment vector* $\mathbf{a_v} = [a_{v,l}]$. If the v^{th} CS is assigned with the l^{th} layer, $a_{v,l}$ is set as 1; otherwise, the $a_{v,l}$ is set as 0. For instance, if the base and the 1st enhanced layer is assigned, the $\mathbf{a_v}$ is shown as [1, 1, 0, 0]. Thus, the bit rate assigned to the v^{th} CS, noted as R_v , can be expressed as:

$$R_v = \mathbf{a}_v \mathbf{R}_0 = \sum_{l=1}^{L} a_{v,l} \cdot \delta R_{v,l} \ . \tag{4.13}$$

The dependency among layers of SVC videos is already considered in this assignment vector $\mathbf{a_v}$.

Now we define The average CQI of the v^{th} CS up to time t is evaluated by using the exponentially weighted method as

$$\bar{b}_v(t) = \begin{cases} (1-\rho)\bar{b}_v(t-1) + \rho b_v(t-1) & t > 1 \\ 1 & t = 1 \end{cases} \tag{4.14}$$

where the weighting factor ρ is set as 1/50 to calculate the average real-time CQI [21][22] in our experiments, and thus the averaged slot capacity is $C_v^{avg}(t) = 9.6 \times \bar{b}_v(t)$ Kbps/slot [15], as shown in Table 2.1. This value is instrumental in the task of estimating the average slot required when the l^{th} layer are assigned to a CS by the BS. For the video with l layers to be uploaded, i.e., the total rate $R_{v,l}$, the average number of slots required is $G_{v,l} = \lceil R_{v,l}/C_v^{avg} \rceil$. For a SVC video, the change of slot demand due to change of video layer assignment from l–1 to l is noted as $\delta G_{v,l} = G_{v,l} - G_{v,l\text{-}1}$ and $G_{v,0}$ is defined as zero. Thus, the average number of slots needed by the v^{th} video can be expressed as:

$$G_v = \sum_{l=1}^{L} a_{v,l} \cdot \delta G_{v,l} \ . \tag{4.15}$$

In the OFDMA system, the total number of slots available at each OFDMA frame is caped at G_0 slots. Hence, the radio resource constraints can be represented by (4.16):

$$\sum_{v=1}^{V} G_v = \sum_{v=1}^{V} \sum_{l=1}^{L} a_{v,l} \cdot \delta G_{v,l} \le G_0 \tag{4.16}$$

Now we define $u_{v,l}$ to be the cumulative video quality gain when up to the l^{th} layer of the v^{th} video is successfully uploaded and received by a subscriber on the DL, where $u_{v,l} > u_{v,l-1}$. Note that the $u_{v,l}$ can also be viewed as $u_{v,l}(r_v)$, where r_v is the rate assigned to the scheduled v^{th} CS. According to [50]-[52], $u_v(r_v)$ is non-decreasing with respect to r_v. Once there are V scalable videos, with L layers in each video, to be uplinked to the web platforms and distributed by multicasting, the total utility U, reflecting the total subscribers' experience or satisfaction for this video, can be expressed as:

$$U = \sum_{v=1}^{V} \sum_{l=1}^{L} \left(N_{v,l} \cdot \delta u_{v,l} \right) \cdot a_{v,l} = \sum_{v=1}^{V} U_v, \tag{4.17}$$

where $\delta u_{v,l} = u_{v,l} - u_{v,l-1}$ is the video quality gain when the l^{th} layer is uploaded and $u_{v,0}$ is defined as zero; U_v is the long term utility to be generated by v^{th} CS.

Eqs. (4.16) and (4.17) lead to the following problem formulation:

P1. A Long Term Video Layer Assignment Problem

Given $\mathbf{R}_0$, $N_{v,l}$, b_v , *and* $\delta u_{v,l}$, *find the assignment* $\mathbf{a}_v = [a_{v,l}]$ for all CSs *that maximizes the total long term utility U defined in* (4.17). *This can be expressed as*

$$\max \ U = \sum_{v=1}^{V} U_v \ ,$$

subject to the constraints in (4.16) *and*

$$1 \le \sum_{l=1}^{L} a_{v,l} \le L, \quad 1 \le v \le V. \tag{4.18}$$

It implies that each CS will be assigned to a designated bit rate, i.e., at least the base layer has to be assigned to a CS to ensure the minimum quality for each UL video. The solution to **P1** is the assignment $\{\mathbf{a}_v^*\}$ for all V CSs. It will then be substituted into (4.13) to calculate the optimal bit rate assignment for each CS as:

$$R_v^* = \mathbf{a}_v^* \mathbf{R}_0 = \sum_{l=1}^{L} a_{v,l}^* \cdot \delta R_{v,l}$$

Further, the video quality assignment, i.e., the targeted video quality, for each CS can be noted as:

$$u_v^* = \sum_{l=1}^{L} a_{v,l}^* \cdot \delta u_{v,l}. \tag{4.19}$$

Thus, the targeted utility of each CS can be expressed as

$$U_v^* = \sum_{l=1}^{L} \left(N_{v,l} \cdot \delta u_{v,l} \right) \cdot a_{v,l}^*.$$

Problem P1 (Eqs. (4.16) and (4.17)) is the classical 0-1 knapsack problem with additional constraints described in (4.18), which has the worst case complexity L^V.

4.3.b Real-Time Packet Scheduling for Assigned Video Layers

The assignment result $\mathbf{a}_v^*$ above yields an optimal targeted average bit rate assignment R_v^* and an optimal targeted utility U_v^* for each CS. The video streams are also allocated with G_v^* slots in each OFDMA frame. However, the assignment result does

Table 4.1: List of Notations

Notation	Description
v	Index of a video program
l	Index of a video layer
L	Total number of layers in each video
L_v	Number of video layers allowed to be uploaded
N_v	Total number of subscribers to the v^{th} video
$N_{v,l}$	Number of subscriber that will receive v^{th} video up to l^{th}
$C(m)$	Slot capacity (Kbps/slot) of m^{th} MCS
b_n / b_v	CQI of a DL subscriber n / UL camera v
$\mathbf{a}_v$ /$a_{v,l}$	Assignment vector/element
$\delta u_{v,l}$	utility gain for l^{th} layer in v^{th} video
$\delta R_{v,l}$	Payload (Kbps) of l^{th} layer in v^{th} video program
G_0	Total available slots for UL in an OFDMA frame
G_v	Avg. number of slots needed to UL v^{th} video
$T_{v,max}$	Tolerable delay for real-time video packet
U	Total utility value

not bind the CS to any particular slot of any specific SCH (frequency band). Besides, for live video streaming, each packet has a deadline ($T_{v,max}$) and should be delivered before the $T_{v,max}$. Otherwise, it will be discarded and resulting in utility degradation. Thus, to achieve the targeted U_v^*, an effective packet scheduler is also essential. The objectives of real time packet scheduler is to (a) decide which CSs should be scheduled in each OFDMA frame, and (b) assign the SCHs and slots to each selected CS such that the real time constraints are met, and the average bit rates will be as close to those targeted R_v^* as possible so that the U_v^* can be reached and the P1 can thus be comprehensively solved. More specifically, in our work, after P1 is solved and the assignment result $\mathbf{a}_v^*$ is obtained, the packet scheduler is to reach the targeted U_v^* found in P1 and will not change the

determined P1 solution; therefore, the real-time packet scheduling is regarded as a finer search for detailed parameters.

All notifications used are conveniently summarized in Table 4.1.

4.3.c DL Resource Management Problem for Layered Video Multicasting

In our integrated framework, the DL resource allocation problem has been discussed in the section 4.2a. This problem is formulated and optimized by using two key steps: 1) optimization on mandatory video base layer and 2) optimization on optional video enhancement layers. Please refer to the section 4.2a for more details.

To efficiently deal with the optimization task formulated in P1, a systematical cross-layer algorithm, named Integrated Visual-Quality-Driven (*IVQD*) Scheduling is proposed, as shown in Figure 4.5. This method intelligently considers the interaction between the APP and MAC/PHY layers so as to optimize the overall utility and concurrently each UL video's quality. Further discussions for *IVQD* are detailed in the following Section 4.4.

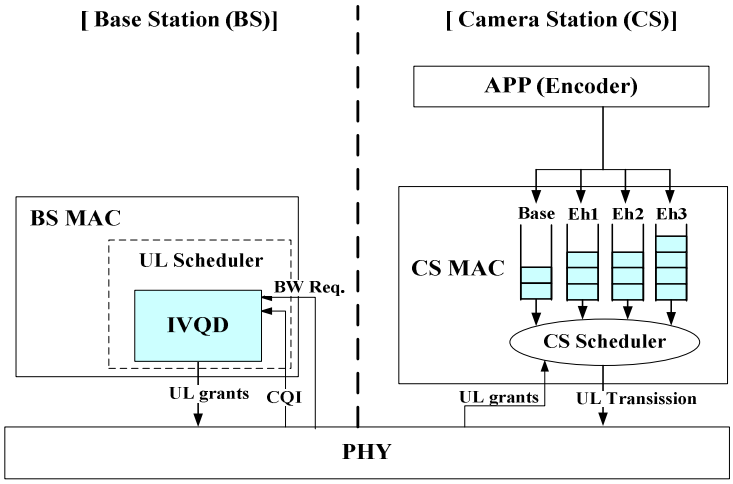

Figure 4.5: The *IVQD* System: In BS, the *IVQD* module is for visual quality optimization. In CS, scalable video with 4 layers is adopted in this example.

4.4 Cross Layer Scheduling and Resource Allocation

4.4.a Long-term Uplink Layers Assignment:

To solve the problem of **P1**, we first define per-slot utility gain $\eta_{v,l}$ as follows:

$$\eta_{v,l} = \frac{N_{v,l} \cdot \delta u_{v,l}}{G_{v,l} - G_{v,l-1}} = \frac{\delta U_{v,l}}{\delta G_{v,l}}; \quad 1 \le l \le L \ , \tag{4.20}$$

where $\eta_{v,l}$ is the unit utility gain when video stream v is assigned with the l^{th} video layer. For a video stream, the change of utility value due to change of video layers from $l-1$ to l is noted as $\delta U_{v,l} = N_{v,l} \cdot \delta u_{v,l}$, and the change of slot demand is $\delta G_{v,l}$, as defined in (4.15). After incremental unit utility gain $\eta_{v,l}$ is defined, we can rewrite (4.17) as follows:

$$U = \sum_{v=1}^{V} \sum_{l=1}^{L} \delta G_{v,l} \cdot \eta_{v,l} \cdot a_{v,l} \tag{4.21}$$

Denote U_{max} to be the maximum utility that can be achieved with G_0 or fewer slots. Clearly, the per unit utility gain U_{max}/G_0 will also be the largest. This observation leads to the first two steps of the bit rate, i.e., video layer, assignment heuristic algorithm. The algorithm proceeds with layer assignment as follows.

Step 1. Compute and then sort $\{\eta_{v,l}; 1 \le v \le V, 1 \le l \le L\}$ to yield a mapping of index (v, l) to an ordered list $\{(v'(f), l'(f)); 1 \le f \le F\}$ such that

$$\eta_{v'(1),l'(1)} \ge \eta_{v'(2),l'(2)} \ge \cdots \ge \eta_{v'(F),l'(F)},$$

where f is the rank index for ordered list and $F = V \times L$.

Step 2. Set $G_u(0) = 0$

For f= 1 to F,

Compute $G_u(f) = G_u(f-1) + \delta G_{v'(f),l'(f)}$

If $G_u(f) \le G_0$,

set $a_{v'(f),l'(f)} = 1$

Else $G_u(f) = G_u(f-1)$

$J = f - 1$, then break the for loop

End for loop

Step 3.

For $f^* = J+1$ to F,

$$\text{If } \delta U_{v'(f^*),\, l'(f^*)} > \sum_{f=1}^{J} \delta U_{v'(f),\, l'(f)}$$

(i) reset $\{a_{v'(f),\, l'(f)} = 0 , G_u(f)=0 ; 1 \quad f \quad J\}$

(ii) set $a_{v'(f^*),l'(f^*)} = 1$

(iii) Redo ***Steps 1*** and ***2*** for the rest (v, l) with

$G_u(0) = \delta G_{v'(f^*),l'(f^*)}$

End for loop

If $G_u(J) < G_0$, perform ***Steps*** 4 and 5. Otherwise, exit.

With ***Steps*** *1* and *2* in this greedy heuristics, each video stream is assigned with the most efficient transmission video layer in terms of utility value per slot, starting from the most efficient video stream. Note that not all videos may be assigned with enhancement layers.

Step 3 guarantees the algorithm performance by preventing any extremely high utility video with lower per slot usage from being discarded.

On the other hand, there are cases when $G_u(J) < G_0$. Under the circumstances, even though each video stream is assigned a bit rate having maximum unit utility gain, there might be some slots left. Hence, it is feasible to transmit more layers for some UL CSs to maximize the overall utility. To do this, the *IVQD* applies the OLM, a DL multicast algorithm [13], to search the CSs to transmit more layers.

For instance, when layer l_t of the v_t^{th} video, noted as (v_t, l_t), is not yet scheduled, the current total utility obtained from ***Steps 1*** to ***3*** is U_T. But when (v_t, l_t) is also put into UL scheduling consideration, the total utility may be increased to U_{T^*} under the same slots constraint. The additional utility gain, defined as $U_{T^*} - U_T > 0$, is obtained because (v_t, l_t) may be the layer resulting in higher utility. Note that the OLM is able to create higher U_T *noted as* U_{T^*} when given the additional choice of (v_t, l_t) for the DL scheduling selection, since it is able, as has been proven, to provide the optimal DL utility when more video layers are given. The selection procedures are detailed in ***Steps 4*** and ***5***.

Step 4.

Find each CS's highest scheduled layer obtained from ***Steps*** *1* to *3* by

$L_v(v)=\{\sum_l a_{v,l}\ ;\ 1 \le l \le L\}$. Next, for all non-selected layers $(L_v(v)+1)$, where $1 \le L_v(v)+1 \le L$, sort$\{\delta U_{v, Lv(v)+1}\ ;\ 1 \le v \le V\}$ to yield a mapping of index v to an ordered list $\{v''(q'');\ 1 \le q'' \le V\}$, such that

$$\delta U_{v''(1),\, Lv(v''(1))+1} \geq \delta U_{v''(2),\, Lv(v''(2))+1} \geq \cdots \geq \delta U_{v''(V),\, Lv(v''(V))+1}.$$

Further, map all scheduled layers from ***Steps** 1* to ***3*** to a list $\{(v^*(f'), l^*(f')); 1 \leq f' \leq J\}$.

***Step 5*.**

For $q'' = 1$ to V,

Find DL layers by OLM, given scheduling selections $\{(v^*(f'), l^*(f')); 1 \leq f' \leq J\}$ and $(v''(q''), L_v(q'')+1)$

If $\delta U_{v''(q''),\, Lv(q'')+1} > \sum_{x=1}^{X} \delta U_{v^*(f''(x)),\, l^*(f''(x))}$

Compute $\delta G = \delta G_{v''(q''),\, Lv(q'')+1} - \sum_{x=1}^{X} \delta G_{v^*(f''(x)),\, l^*(f''(x))}$

If $G_u(J)+\delta G \leq G_0$

set $a_{v''(q''),\, Lv(q'')+1} = 1$.

$\{a_{v^*(f''(x)),\, l^*(f''(x))} = 0 \; ; \; 1 \leq x \leq X\}$

$G_u(J) = G_u(J)+\delta G$

$J \leftarrow J - X + 1$

Then redo Step 4 and 5.

End if

End if

End for loop

More specifically, the video layer assignment problem is now solved by searching the layers with maximum unit utility gain within the slots constraint. The proposed *IVQD* method improves the uplink video delivery of CSs towards the highest possible DL utility

by incorporating the OLM algorithm. Besides, by using the OLM, the integrated system can evaluate the number of MSs which can receive a specific layer, i.e. $N_{v,l}$, and the value of $\delta U_{v,l}$ based on the feedback information, such as CQI, of DL users. The *IVQD* principle above is summarized in Fig. 4.6.

The complexity of *IVQD* algorithm above can be assessed as: Line 4 and 5 take $O(N_v)$ [4] and $O(VL)$ operations respectively. Line 7 has $O(VL \cdot logVL)$ operations for sorted scheduling in ***Step*** 1 and 2. Then, in the ***Step*** 3, it may have $O(VL)$ as the highest amount of operations. After these steps, the worst case for ***Step*** 4 and 5 is $O(N_v VL)$ and $O(VL \cdot logVL)$ respectively. Thus, the overall complexity in Figure 4.6 is MAX$\{O(N_v)$, $O(N_v VL)$, $O(VL)$, $O(VL \cdot logVL)\} = O(VL \cdot logVL)$. It is therefore reasonable to assume that the *IVQD* layer allocation algorithm is suitable for real time implementation.

1: **Repeat** every ε seconds
2: Update the channel quality for all V CSs
3: **for** all eligible (v, l) **do**
4: (i). Use OLM in [13] to evaluate the $N_{v,l}$ and $\delta U_{v,l}$
5: (ii). Then find $\eta_{v,l}$.
6: **end for**
7: Schedule all (v, l) by using ***Step*** **1** to **3** until no available slots subject to layer dependency
8: **If** there are unscheduled layers && $G_u(J) < G_0$
9: Based on ***Step 4*** and ***5***, find the higher utility by OLM
10: Update the layer assignment results
11: **end** If until all layers are tested
12: **until** end of video session

Figure 4.6: Pseudo code for video layer assignment in *IVQD* algorithm.

4.4.b Frame-by-Frame Real-Time Packet Scheduling

Once the scheduling of individual video layer is determined from Sec. 4.4.a, the video packets associated with the scheduled layer need to be effectively allocated in each OFDMA frame. The utility-based priority scheduling for each CS is adopted for scheduling packets frame-by-frame. Based on the unit utility gain and the queuing delay, the BS scheduler calculates the priority of each CS and serves them according to their priority in descending order. The priority function defined is

$$\phi_{v,k}(t)=\begin{cases}\frac{U_{v,\,norm}}{s_{v,\,k}}\frac{1}{F_v} & ,\text{if } F_v(t)\geq 1 \text{ and } b_{v,k}(t)\neq 0\\ 1 & ,\text{if } F_v(t)<1 \text{ and } b_{v,k}(t)\neq 0\\ 0 & ,\text{otherwise,}\end{cases} \tag{4.22}$$

where

$$U_{v,norm}=\sum_{l=1}^{L}\left(N_{v,l}\cdot\delta u_{v,l}\right)\cdot a_{v,l}\Big/U \tag{4.23}$$

and

$$F_v\,(t)=(T_{v,\max}-W_v(t))/T_s \tag{4.24}$$

The $\phi_{v,k}$ is the priority of the v^{th} CS on k^{th} SCH and $U_{v,norm}$ is the normalized utility. The $s_{v,k}=\lceil R_v/C_{v,k}\rceil$ is the estimated slots consumption when CQI is $b_{v,k}$. F_v is the delay factor [3] with $T_{v,max}$ and W_v denotes the maximum tolerable delay and waiting time respectively. T_s is the guard time and usually is the same as the scheduling period. When F_v<1, it means the queue in the v^{th} CS has the packet with delay approaching the $T_{v,max}$ and should

be served immediately. This mechanism can effectively decrease the packet loss while maintaining the users' satisfaction.

The steps for packet scheduling are as shown below:

1. For each UL CS, get the ranking list of priority $\{\varphi'_s\}$ for all the K SCHs by using (4.22):

$$Q_v = \{k_1, k_2, ..., k_K : \phi_{v,k_1} \geq ... \geq \phi_{v,k_K}\}; \quad v = 1, ..., V \tag{4.25}$$

The $\varphi_{v,k}$ will be deleted from the Q_v once there is no available slot for UL video transmission in the k^{th} SCH.

2. Get the highest φ for each CS and defined it as P_v, which is the maximum in Q_v

$$P_v = \max\{Q_v\}; \quad v = 1, 2, ...V \tag{4.26}$$

3. For The CS v^{sch} which has the maximum P_v will be scheduled and allocated to the available SCH k^{sch} where:

$$(v^{sch}, k^{sch}) = \arg\max_{(v,k)}\{P_v\}; \tag{4.27}$$

The instant CQI assigned to v^{sch} at frame t can be shown as

$$b_{v^{sch}}(t) = b_{v^{sch},k^{sch}}(t) \tag{4.28}$$

This assigned CQI can be mapped to the corresponding MCS m, as shown in Table 4.1, and the MCS adopted by CS v^{sch} is thus obtained. The average CQI is updated by (4.14).

In our system, we iteratively schedule the CS and select the assigned SCH along with the corresponding MCS by using the step 1, 2, and 3 above in every OFDMA frame until no more slots are available or all CSs have been served.

The complexity of *IVQD* packet scheduler is assessed as follows: In (4.25), for each CS, the priority in (4.22) needs to be evaluated for all K SCHs and these K results in turn need to be sorted. Thus (4.25) has $O(VK) + O(VK \cdot logVK)$ operations. As regards (4.26) and (4.27), both require $O(V)$ operations. So the overall complexity is $\text{MAX}\{O(VK), O(VK \cdot logVK), O(V)\} = O(VK \cdot logVK)$. It is hence justifiable to apply the proposed scheduler to real-time application.

4.5 Simulation and Performance Comparison

4.5.a Utility-Driven Greedy Algorithm

The performance of the proposed *IVQD* algorithm is evaluated through extensive simulations. Specifically, the performance of *IVQD* algorithm and a baseline Utility-Driven Greedy algorithm [16][17] are compared over a number of different scenarios. More details about Utility-Driven Greedy have been already introduced in Sec. 3.5.a. To validate the near-optimal performance of the *IVQD* algorithm, exact globally optimal solution will be computed using exhaustive search.

4.5.b Simulation Configuration

In this paper, the simulations are performed according to [20][27]. The simulated WCN includes two WiMAX cells, with a BS for uplink and the other for downlink. Each BS is set in the center of its cell and the connected UL CSs and DL MSs are uniformly distributed within their cells. The channel propagation loss is estimated based on the COST 231 sub-urban model and the small scale fading effect is measured employing the ITU Vehicular A multipath model [27]. Our simulated system is set to work on a 10 MHz band with a 5ms OFDMA frame [27]. For UL transmission, the band-AMC permutation mode [20] is adopted. In the DL cell, the PUSC mode is used for video multicast. The configuration for the system parameters in the simulation are summarized in Table 3.2, and the parameters of OFDMA band-AMC and PUSC mode are shown in Table 3.3 and Table 4.2 respectively.

Table 4.2: PUSC OFDMA Parameters

Parameters	Value
Permutation mode	PUSC
FFT size	1024
Sub-carrier frequency spacing (f)	10.94 kHz
Useful Symbol Time ($T_b = 1/f$)	91.4μs
Guard time ($T_g = T_b /8$)	11.4 μs
OFDMA Symbol Duration ($T_g = T_b + T_g$)	102.9 μs
Frame duration (t_{fr})	5 ms
Band-AMC Mode	
Null sub-carriers	184
Pilot sub-carriers	120
Data sub-carriers	720
Number of Sub-carrier per cluster	24 data + 4 pilot
Number of clusters per slot	2

UL scenario: A cell with 6 uniformly distributed UL CSs is considered. Each CS provides a live video, which is SVC coded with L = 4 layers (1 base + 3 enhancement layers), and the corresponding utility gain for 4 different layers are set as $\delta u_{v,l}$ ={0.5, 0.25, 0.15 0.1}. Each layer has an identical rate $\delta R_{v,l}$ = 250 Kbps for all v and l. Thus, each video consumes an aggregate rate of 1 Mbps. Further, the maximum latency of $T_{v,\max}$ = 50 ms queuing, defined in (4.24), for each UL packet is used to determine packet loss.

There are three UL algorithms to be compared: 1) the Exhaustive search for globally optimal solution, 2) the proposed *IVQD* method, and 3) the Utility-driven Greedy algorithm. Each method needs to decide the number of uploaded layer for the v^{th} video, i.e., L_v. On the DL, the utility produced by each video is feedback to each UL CS every 5 secs [16] and treated as the resource allocation indicator.

To evaluate the users' satisfaction by each UL algorithm, we compare their total utility and the normalized utility produced by all CSs under two different amounts of resource reserved for UL video aggregations: a) 154 slots and b) 132 slots. The case of (b) represents a situation where the resources are scarce in view of the size of the payload.

DL scenario: On the DL, the OLM is applied to obtain the optimal multicast utility [13]. Further, 6 UL videos are requested by groups of MSs, with the number of multicast subscribers for each UL video being N_v = [100, 90, 80, 60, 40, 20]. Besides, 330 slots are reserved for DL videos per OFDMA frame.

Table 4.3: The average utility value in 20 secs. N_v = [100, 90, 80, 60, 40, 20]

	G_0=132	G_0=154
	Utility	Utility
Exhaustive	360.0156	368.54
IVQD	360.0078	364.17
Greedy	327.96	355.93

Table 4.4: The average utility value every 5 secs by each method and 20 secs overall. Stage 1 = 0~5 sec, Stage 2 = 6 ~ 10 sec and so on. N_v = [100, 90, 80, 60, 40, 20]

	G_0=132			
	Stage1	Stage2	Stage3	Stage4
Exhaustive	362.64	358.93	358.83	359.66
IVQD	362.64	358.90	358.83	359.66
Greedy	322.85	328.19	329.80	330.995

Table 4.5: The average utility value every 5 secs by each method and 20 secs overall. Stage 1 = 0~5 sec, Stage 2 = 6 ~ 10 sec and so on. N_v = [100, 90, 80, 60, 40, 20]

	G_0=154			
	Stage1	Stage2	Stage3	Stage4
Exhaustive	368.69	367.60	368.61	369.22
IVQD	368.60	362.59	362.43	363.05
Greedy	348.59	354.38	359.15	361.58

4.5.c Simulation Results

The experiment results for the overall system performance are summarized in Table 4.2, 4.3, and 4.4. Each entry in Table 4.2 displays the mean of utility values over 20 seconds, and that of every 5 seconds in Table 4.3 and 4.4. It can be seen that, compared with the optimal value by exhaustive method, the total utility by proposed algorithm is very close to the optimal utility in these tables, especially when G_0 =132. It further demonstrates that the resource usage efficiency needs to be considered while searching for the solution of the optimal system performance.

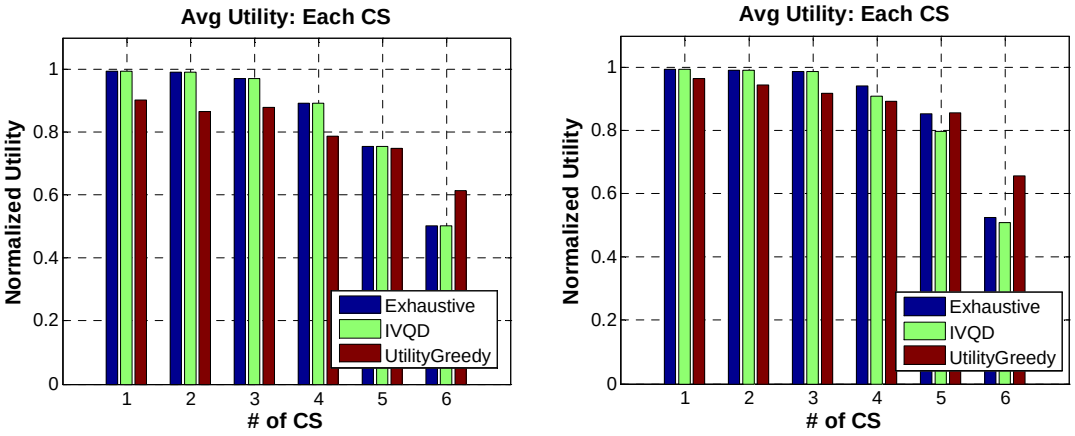

(a). (b).

Figure 4.7: (a). Normalized utility of each CS when (a) G_0=132. (b) G_0= 154.

In addition to the total utility created by each method, we are also interested in the utiltiy of each video. Figure 4.7 shows the comparison of each individual CS operated by optimal, *IVQD*, and Greedy algorithms separately. The normalized utility is used to reflect the obtained satisfaction from the subscribers of a specific video, i.e.,

$$\overline{U_v} = \sum_{l=1}^{Lv} u_{v,l} N_{v,l} \Big/ \sum_{l=1}^{L} u_{v,l} N_v \qquad (4.29)$$

This is the ratio of the expected utility gain when the L_v video layers are scheduled to the maximum possible utility when all L video layers are scheduled. Figure 4.8 and 4.9 also show the cumulative utility over time for the most popular video (CS1) and the least popular video (CS6). Compared with the Greedy method, the *IVQD* algorithm provides higher utility for the more popular videos (such as CS1-CS4). For the less popular videos (such as CS5-CS6), *IVQD* guarantees its basic utility and prevents quality downgrading due to the change of scheduling decision or channel fading. The situations are identical in both radio resource budget scenarios.

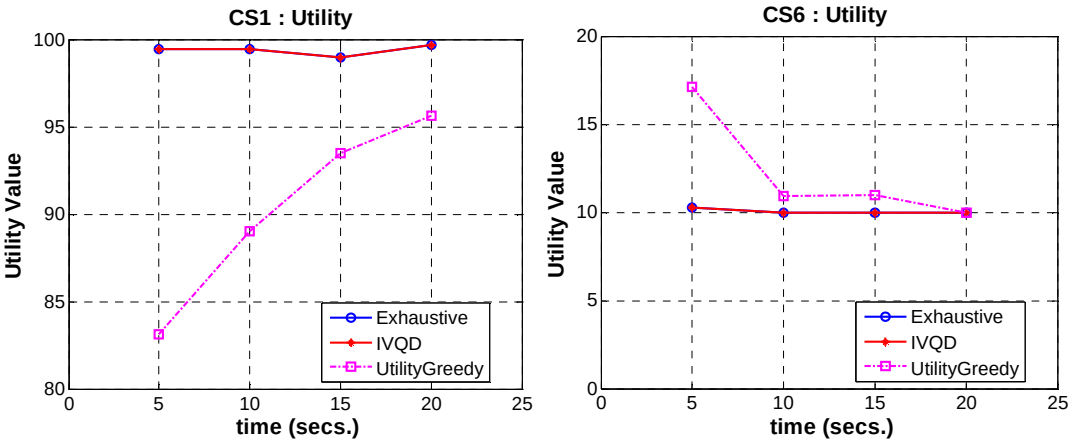

(a). (b).

Figure 4.8: Utility generated by (a). CS1 (b). CS6 using 3 methods . G_0= 132

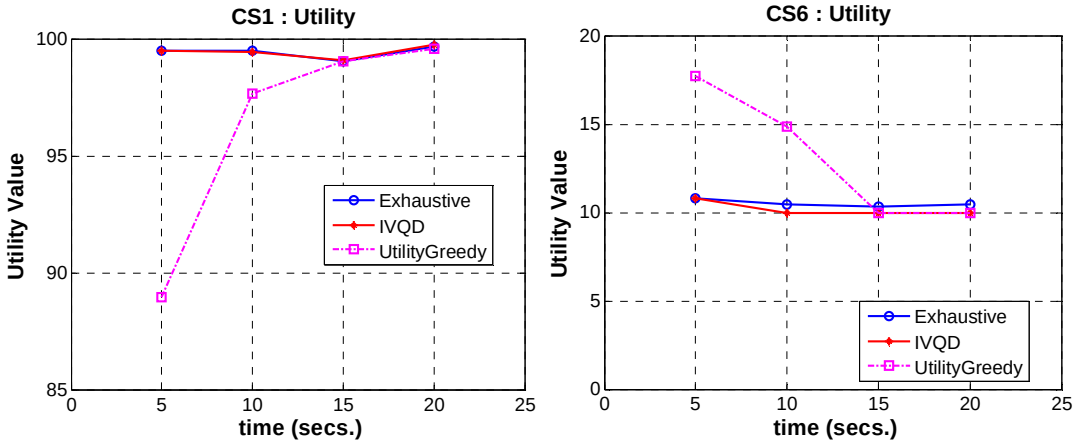

(a). (b).

Figure 4.9: Utility generated by (a). CS1 (b). CS6 using 3 methods. G_0= 154.

Figures 4.10(a) and 4.10(b) further show respectively the packet loss rate of CS1 and CS6 by the three methods. Compared with the Utility Greedy scheme, Figures 4.9(a) and (b) show that, even when the available resource is reduced, the *IVQD* still maintains good performance on loss rate for each CS.

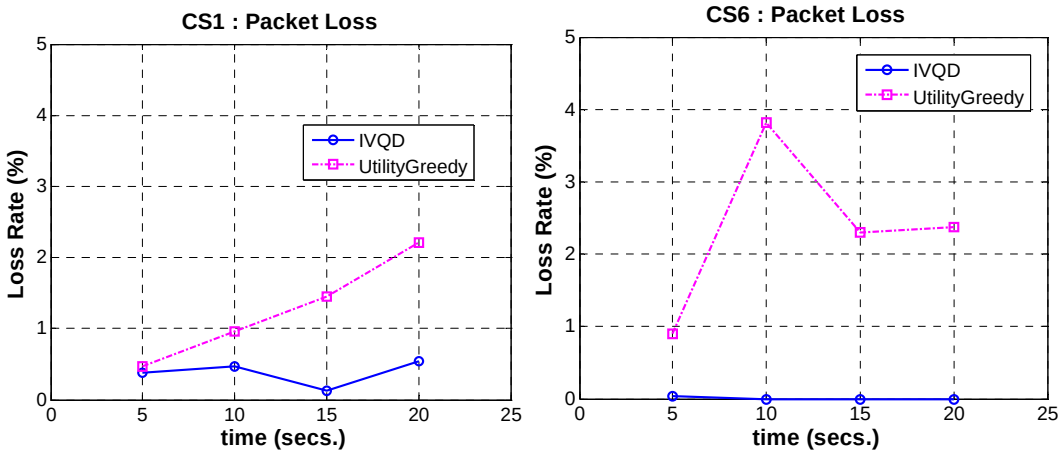

(a). (b).

Figure 4.10: Packet loss rate of 2 methods on (a). CS1 and (b). CS6 when G_0= 132.

Chapter 5 – Conclusion and Future Works

In this dissertation, we comprehensively proposed a novel and effective cross-layer scheduling and resource allocation algorithm for real-time video camera networks over the OFDMA-based wireless infrastructure. The scenarios including real-time unicast video uplinking, layered video multicasting, and video transmission in an integrated UL and DL system are all investigated within two major applications of our research: real-time surveillance video UL delivery and user-generated video transmission, from video content generators to subscribers, through the UL and DL integrated systems.

For the real-time surveillance video system, we are proposing a novel *VQD* algorithm that yields near-optimal solutions to both the long term bit rate assignment and the real-time packet scheduling for the uplink wireless multimedia system over the mobile network of next generation. This method determines the most appropriate video encoding rate for all videos by considering each CS's utility, reflecting the video perceived quality along with the importance of video content, and the channel quality. Further, the packet scheduler proposed in *VQD* solution, considering each CS's average received rate, HOL delay, instantaneous CQI, and unit utility gain and incorporating with a efficient resource allocation policy to determine the number of slots to be assigned, is applied to select best set of CSs uploading their video packets in each OFDMA frame. It is also shown to be capable of exploiting the inherent diversity gain due to wireless channel variation.

For the integrated system, in view of rapid fluctuating channel conditions for UL CSs and DL subscribers, the proposed *IVQD* algorithm adopts layer-encoded video

technology to facilitate more flexible and robust data rate adaptation. On the DL side, *IVQD* algorithm employs the OLM scheduling, a previously proposed video multicast algorithm, to optimize the DL performance. For each video layer successfully uplinked, the OLM selects the best subset of MSs to receive this layer to maximize the total utility and assigns the most efficient MCS to transmit the data.

The *IVQD* algorithm determines the number of video layers to be uploaded by jointly considering each UL CS's channel quality and the video perceived quality from all DL subscribers. To obtain the best set of video layers optimizing the total utility, it combines with the OLM method to further search adequate UL CSs to transmit more layers under the resource constraint. To optimize the real-time UL scheduling, the *IVQD* also proposed a packet scheduler, considering each CS's HOL delay, instantaneous CQI, to select best set of CSs uploading their video packets in each OFDMA frame. Besides, to apply the *IVQD* method to the real system, we further use the OLM to estimate the possible number of receivers and potential utility to be generated for each video layer based on all DL MSs' latest CQI feedback.

The simulation results indicate that both *VQD* and *IVQD* are able to deliver superior performances in a good many aspects, including higher spectrum efficiency and throughput, much lower packet loss, more stable video quality, higher enhanced utility, etc. as compared with the baseline methods. This proposed system can be applied to various real-time monitoring scenarios and is readily applicable to any OFDMA 4G technologies, such as WiMAX and LTE.

In view of the practical limitations of feedback resource for mobile uplink systems, we presented the packet schedulers using only the allowable number of the actual feedback information from CSs, such as HOL and bandwidth request, in the OFDMA systems. The first future work is to apply the proposed scheduler to LTE type of networks, which use SC-FDMA in the uplinking, and will require different radio resource allocation policy. Further extension of this work resides in adopting more information from videos, such as the type of video frame, to adjust the scheduling priority, e.g., the I-frame packets in a higher weighted CS should have the higher priority than P-frame packets of others. In addition, the design for scheduler in mobile CS, allocating the bandwidth required from a BS to adequate packets in its queue for uploading, should be worth investigating as well.

Moreover, to efficiently deliver the multimedia content to multiple destinations, the 3GPP LTE has also introduced the Multimedia Broadcast/Multicast Service (MBMS) as a mean to broadcast and multicast information to 3G and 4G users. However, its performance is still restricted by the following factors:

1) The performance of user terminals (UEs) at the overlapping cellular regions could be effected by destructive interferences (i.e., Inter-Symbol Interference (ISI)).

2) The performance of a MS gradually degrades as it moves away from the BS.

MBSFN (MBMS over a Single Frequency Network) has therefore been proposed for LTE [69] to improve the performance of MBMS. In the MBSFN technology, all the BSs transmit the same signal at the same time and over the same frequency channel to users. As a result, the BSs are required to be tightly time-synchronized. In this case, the

transmissions received from multiple cells will, as seen from the UE, appear as a single transmission subject to severe multipath propagation. It thus overcomes the two mentioned shortcomings of MBMS by transforming destructive interference to constructive interferences [70][71][72] and potentially enhances quality of mobile video service over OFDMA-based 4G networks [45]. Therefore, a natural continuation for OLM algorithm should be applying it to the MBSFN structure, which will require new criterion for MCS selection and FEC configuration.

Bibliography

[1] J.-N. Hwang. *Multimedia Networking: From Theory to Practice.* Cambridge University Press, 2009

[2] J. -N. Hwang and V. Gau, “Tracking of Multiple Objects over Camera Networks with Overlapping and Non-overlapping Views,” Chap. 7, Distributed Video Sensor Networks, Springer, 2011

[3] L. Wan, W. Ma, Z. Guo, “A Cross-layer Packet Scheduling and Subchannel Allocation Scheme in 802.16e OFDMA System,” in *Proc. IEEE WCNC 2007*, Mar. 2007, pp. 1867-1872

[4] Q. Liu, X.Wang, and G.-B. Giannakis, ”A Cross-Layer Scheduling Algorithm with QoS Support in Wireless Networks,” *IEEE Trans. on Veh. Technol.*, vol. 55, no. 3, pp. 839-847, May 2006

[5] X. Zhu, J. Huo, X. Xu, and C. Xu, “QoS-Guaranteed Scheduling and Resource Allocation Algorithm for IEEE 802.16 OFDMA System,” in *Proc. IEEE ICC 2008*, May 2008, pp. 3463-3468

[6] X. Zhu, J. Huo, S. Zhao, Z. Zeng, and W. Ding “An Adaptive Resource Allocation Scheme in OFDMA based Multiservice WiMAX Systems,” in *Proc. ICACT*, Feb. 2008, pp.593-597

[7] H.- K. Rath, A. Bhorkar, V. Sharma, “An Opportunistic DRR (O-DRR) Uplink Scheduling Scheme for IEEE 802.16-based Broadband Wireless Networks,” in *Proc. ICNGN*, Mumbai, Feb. 2006

[8] P. Viswanath, D.- Tse, R. Laroia ”Opportunistic Beamforming Using Dumb Antennas,” *IEEE Trans. on Inform. Theory*, Vol. 48, No. 6, pp. 1277-1294, June 2002

[9] P.-H. Wu and J.-N. Hwang, “Cross-Layer Channel-Quality-Fair Scheduling for Video Uplink of Camera Networks over WiMAX,” in *Proc. IEEE ICC*, Kyoto, Japan, June 2011

[10] G. Piro, L. -A. Grieco, G. Boggia, F. Capozzi, and P. Camarda, “Simulating LTE Cellular Systems: An Open-Source Framework,” *IEEE Trans. on Veh. Technol.*, vol. 60, pp. 498-513, Feb. 2011

[11] M. Andrews, K. Kumaran, K. Ramanan, A. Stolyar, P. Whiting, and R.Vijayakumar, “Providing quality of service over a shared wireless link,” *IEEE Commun. Mag.*, vol. 39, pp. 150-154, Feb. 2001

[12] M. Andrews, K. Kumaran, and K. Ramanan, "CDMA Data QoS Scheduling on the Forward Link with Variable Channel Conditions,” *Bell Labs Tech. Memo.*, Apr. 2000

[13] C.-W. Huang, S.-M. Huang, P.-H. Wu, S.-J. Lin, and J.-N. Hwang. “OLM: Opportunistic Layered Multicasting for Scalable IPTV over Mobile WiMAX,” *IEEE Trans. on Mobile Computing*, vol. 11, no.3, pp.453-463, March 2012

[14] W.-H. Kuo, W. Liao, and T. Liu, "Adaptive Resource Allocation for Layer-Encoded IPTV Multicasting in IEEE 802.16 WiMAX Wireless Networks,” *IEEE Trans. on Multimedia*, vol. 13, no. 1, pp 116-124, Feb. 2011

[15] P.-H. Wu and Y.-H. Hu, "Optimal Layered Video IPTV Multicast Streaming over Mobile WiMAX Systems," *IEEE Trans. on Multimedia*, pp.1395-1403, Dec. 2011

[16] S. Thakolsri, S. Khan, E. Steinbach, and W. Kellerer, "QoE-driven cross-layer optimization for high speed downlink packet access," *Journal of Communication*, vol. 4, no. 9, pp.669–680, Oct. 2009

[17] A.- E. Essaili, E.- Steinbach, D.- Munaretto, S.- Thakolsri, and W.-Kellerer, “QoE-driven resource optimization for user generated video content in next generation mobile networks,” in *Proc. IEEE ICIP*, Sep. 2011

[18] A.- E. Essaili, L.- Zhou, D.- Schroeder, E.- Steinbach, and W.- Kellerer, "QoE-driven Live and On-Demand LTE Uplink Video Transmission," in *Proc. IEEE MMSP*, Oct. 2011

[19] P.-H. Wu, J.-N. Hwang, J.-Y Pyun, K.-M. Lan, and J.-R. Chen "QoE-Aware Resource Allocation for Integrated Surveillance System Over 4G Mobile Networks," in *Proc. IEEE ISCAS*, Seoul, Korea, May 2012, pp1103-1106

[20] "IEEE standard for local and metropolitan area networks Part 16: Air interface for broadband wireless access systems," *IEEE Std 802.16-2009*, 2009

[21] J. Wu, J. Mo, and T. Wang, "A Method for Non-Real-Time Polling Service in IEEE 802.16 Wireless Access Networks," in *Proc. IEEE Veh. Technol. Conf.*, Baltimore, MD, 2007, pp 1518-1522

[22] F. Hou, P. Ho, X. Shen, and A. Chen, "A Novel QoS Scheduling Scheme in IEEE 802.16 Networks," in *Proc. IEEE WCNC*, Hong Kong, 2007

[23] J. Huang, V.-G. Subramanian, R. Agrawal, and R. Barry, "Joint Scheduling and Resource Allocation in Uplink OFDM Systems for Broadband Wireless Access Networks," *IEEE Journal on Selected Areas in Commun.*, vol. 27, no. 2, Feb. 2009

[24] C. So-In, R. Jain, and A. Al-Tamimi, "Scheduling in IEEE 802.16e Mobile WiMAX Networks: Key Issues and a Survey," *IEEE Journal on Selected Areas in Commun.*, vol. 27, no. 2, Feb. 2009

[25] G.-M. Yao and B.-H Ryu, "Method for Requesting Resource and Scheduling for Uplink Traffic in Mobile Commun. and Apparatus Thereof," *United States Patent*, US 8363625 B2, Jan. 2013

[26] H. Holma, A. Toskala, *LTE for UMTS: OFDMA and SC-FDMA Based Radio Access*. John Wiley & Sons, 2009

[27] WiMAX Forum, "WiMAX System evaluation methodology V2.1," Jul. 2008

[28] J. G. Andrews, A. Ghosh, and R. Muhamed, *Fundamentals of WiMAX: Understanding Broadband Wireless Networking*. Upper Saddle River, NJ: Prentice Hall, 2007

[29] L. Choi, M. T. Ivrlac, E. Steinbach, and J. Nossek, "Sequence-level methods for distortion-rate behavior of compressed video," in *Proc. IEEE ICIP*'05, Genova, Italy, Sept. 2005

[30] R. Basukala, H. M. Ramli, and K. Sandrasegaran, "Performance analysis of EXP/PF and M-LWDF in downlink 3GPP LTE system," in *Proc. 1st AH-ICI*, Kathmandu, Nepal, Nov. 2009

[31] M. Andrews, L. Qian, A. Stolyar, "Optimal Utility based Multi-User Throughput Allocation Subject to Throughput Constraints," *IEEE INFOCOM*, Mar. 2005

[32] Y. Li, and B. Bhanu, "Utility-Based Camera Assignment in a Video Network: A Game Theoretic Framework," *IEEE Sensors Journal*, vol. 11, no. 3, March 2011

[33] S. Khan, S. Duhovnikov, E. Steinbach, and W.-Kellerer, "MOS-based Multiuser Multiapplication Cross-Layer Optimization for Mobile Multimedia Communication," *Advances in Multimedia, article ID 94918*, Jan. 2007

[34] Final report from the Video Quality Experts Group, "On the validation of objective models of video quality assessment," Oct. 2003

[35] D. Schroeder, A.- E. Essaili, E.- Steinbach, D.- Staehle, and M. Shehada, "Low-Complexity No-Reference PSNR Estimation for H.264/AVC Encoded Video," *International Packet Video Workshop*, San Jose, CA, USA, Dec. 2013

[36] M. Fiedler, T. Hossfeld, and P. Tran-Gia, "A Generic Quantitative Relationship between Quality of Experience and Quality of Service," *IEEE Network*, vol. 24, no.2, Mar./Apr. 2010

[37] R. Stankiewicz, P. Cholda, A. Jajszczyk, "QoX–What is really?," *IEEE Commun. Magazine*, vol. 49, no. 4, Apr. 2011

[38] C. Yim and A.-C. Bovik, "Quality Assessment of Deblocked Images," *IEEE Trans. on Image Processing*, vol. 20, no. 1, Jan. 2011

[39] C. Kiraly, L. Abeni, and R.-L. Cigno, "Effects of P2P Streaming on Video Quality," in *Proc. IEEE ICC*, Cape Town, South Africa, May 2010

[40] Y.-F. Ou, Z. Ma, Huang, and Y. Wang, "A Novel Quality Metric For Compressed Video Considering Both Frame and Quantization Artifacts," *VPQM*, Scottsdale, AZ, Jan 2009

[41] S. Wolf and M. Pinson, "Video Quality Measurement Techniques," NTIA, Tech. Rep. 02-392, Jun. 2002

[42] C. Cicconetti, L. Lenzini, placeE. Mingozzi, and C. Eklund, "Quality of service support in IEEE 802.16 networks," *IEEE Network*, vol. 20,pp. 50-55, April 2006

[43] A. Sayenko, O. Alanen, J. Karhula, and T. Hamaainen,"Ensuring the QoS Requirements in 802.16 Scheduling," *in Proc. Int. Workshop Modeling Analysis and Simulation Wireless and Mobile Systems*, Terromolinos, Spain, 2006

[44] J. Lakkakorpi, A. Sayenko, and J. Moilanen. "Comparison of different scheduling algorithms for wimax base station: Deficit round-robin vs. proportional fair vs. weighted deficit round-robin," *IEEE WCNC*, pages 1991–1996 , March 2008

[45] O. Oyman, J. Foerster, T. Yong-joo, and L. Seong-Choon, "Toward enhanced mobile video services over WiMAX and LTE," *IEEE Communications Magazine*, vol. 48, no. 8, pp. 68–76, Aug. 2010.

[46] C. Lee, K. Song, Y. Joo, and Y. Kim, "Adaptive rate control for real-time video streaming over the mobile WiMAX," *IEEE Asia Pacific Conference on Circuits and Systems (APCCAS)*,Nov. 30 - Dec. 30 2008.

[47] C.-W. Huang, M. Loiacono, J. Rosca, J.-N. Hwang, "Airtime Fair Distributed Cross-Layer Congestion Control for Real-Time Video Over WLAN" *IEEE Trans. On Circuits and Systems for Video Technol.*, VOL. 19, no. 8, August 2009

[48] C.-W. Huang, M. Loiacono, J. Rosca, and J.-N. Hwang, “Distributed cross layer congestion control for real-time video over WLAN,” *in Proc. IEEE Int. Conf. Commun. (ICC 08)*, Beijing, China, pp. 2270–2276. May 2008

[49] *Advanced Video Coding for Generic Audiovisual Services*, ITU-T Rec. H.264 and ISO/IEC 14496-10 (MPEG-4 AVC), ITU-T and ISO/IEC JTC 1, Version 8 (including SVC extension): Consented in July 2007

[50] T. Schierl, T. Stockhammer, and T. Wiegand, “Mobile Video Transmission Using Scalable Video Coding,” *IEEE Trans. Circuits and Systems for Video Technology*, vol. 17, no. 9, pp. 1204-1217, Sept. 2007

[51] H. Schwarz, D. Marpe, and T. Wiegand, “Overview of the Scalable Video Coding Extension of the H.264/AVC Standard,” *IEEE Trans. Circuits and Systems for Video Technology*, vol. 17, no. 9, pp. 1103-1120, Sept. 2007

[52] H. Zhang, Y. Zheng, M.-A. Khojastepour, and S. Rangarajan, “Cross-Layer Optimization for Streaming Scalable Video over Fading Wireless Networks,” *IEEE Journal on Selected Areas in Commun.,* VOL. 28, NO. 3, April 2010

[53] J. She, F. Hou, P.-H. Ho, and L.-L. Xie, “IPTV over WiMAX: Key Success Factors, Challenges, and Solutions,” *IEEE Communi. Mag.*, August 2007

[54] W.-H. Kuo, T. Liu, and W. Liao, “Utility-Based Resource Allocation for Layer-Encoded IPTV Multicast in IEEE 802.16 (WiMAX) Wireless Networks,“ *IEEE ICC*, 2007

[55] S. Deb, S. Jaiswal, and K. Nagaraj, “Real-Time Video Multicast in WiMAX Networks,” *IEEE INFOCOM* , pp. 1579—1587, April 2008

[56] C.-W. Huang; P.-H. Wu, S.-J. Lin; J.-N. Hwang, "Layered video resource allocation in Mobile WiMAX using opportunistic multicasting," *IEEE WCNC*, 2009

[57] C. So-In, R. Jain, and A. Al-Tamimi, “Capacity Evaluation for IEEE 802.16e Mobile WiMAX,” To appear in *Journal of Comp. Systems, Networks, and Comm. (Special Issue in WiMAX, LTE, and WiFi Internetworking)*, April 2010

[58] Tao Jiang et. al., “Multicast Broadcast Services Support in OFDMA Based WiMAX Systems”, *IEEE Comm. Mag*., August 2007

[59] J. Wang, M. Venkatachalam and Y. Gang, “System Architecture and Cross-Layer Optimization of Video Broadcast over WiMAX”, *IEEE Journal on Selected Areas in Communications*, vol. 25, no. 4, May 2007

[60] D. Tsitserov, G. Markarian, I. Manuylov, “Real-Time Video Distribution over WiMAX Networks,” Proc. *Annual Postgraduate Symposium*, Liverpool, UK 2008

[61] Y.-R. Yang, M.-S. Kim, and S.-S. Lam, “Optimal partitioning of multicast receivers,” *Proc. IEEE ICNP*, Nov. 2000

[62] P.K. Gopala and H. Gamal, “Opportunistic Multicasting,” *Proc. Conf. Record of the 28th Asilomar Conf. Signals, Systems and Computers*, vol. 1, Nov. 2004.

[63] W. Ge, J. Zhang, and S. Shen, “A Cross-Layer Design Approach to Multicast in Wireless Networks,” *IEEE Trans. Wireless Comm.*, vol. 6, no. 3, Mar. 2007.

[64] U. Kozat, “On the Throughput Capacity of Opportunistic Multicasting with Erasure Codes,” *Proc. IEEE INFOCOM*, pp. 520- 528, Apr. 2008.

[65] Q. Qu and U. Kozat, “On the Opportunistic Multicasting in OFDM-Based Cellular Networks,” *Proc. IEEE ICC*, pp. 3708-3714, May 2008.

[66] P.-H. Wu, Y.-H. Hu, and J.-N. Hwang, “Optimal Layered Video IPTV Multicast Streaming over IEEE 802.16e WiMAX Systems,” *Proc. IEEE VTC2010-Spring*, Taipei, Taiwan, May 2010

[67] S.-M. Huang, J.-N. Hwang, and Y.-C. Chen, “Reducing Feedback Load of Opportunistic Multicast Scheduling over Wireless Systems,” *IEEE Comm. Letters*, vol. 14, no. 12, Dec. 2010

[68] H. Lee, S. Lee, “Definition of a new service class, artPS for video services over WiBro/Mobile WiMAX systems, ” *Springer Journal Wireless Networks*, VOL. 11, Issue 1, January 2011

[69] 3GPP TS 25.346, ”*Introduction of the Multimedia Broadcast Multicast Service (MBMS) in the Radio Access Network (RAN); Stage 2 (Release 8)*”, V8.0.0, December 2007.

[70] L. Rong, O. Haddada, and S. Elayoubi, "Analytical Analysis of the Coverage of a MBSFN OFDMA Network," *Proc. IEEE GLOBECOM 2008,* New Orleans, LO, USA, Nov./Dec. 2008

[71] A. Alexiou, C. Bouras, V. Kokkinos, A. Papazois, and G. Tsichritzis,“Spectral Efficiency Performance of MBSFN-enabled LTE Networks,” *IEEE WiMob 2010*, Niagara Falls, Canada, pp. 361-367, 2010.

[72] A. Alexiou, C. Bouras, V. Kokkinos and G. Tsichritzis, “Communication Cost Analysis of MBSFN in LTE,” *Proc. IEEE PIMRC'10*, Istanbul, Turkey, 2010.

[73] J. J. Ramos-Munoz, J. Prados-Garzon, P. Ameigeiras, J. Navarro-Ortiz, and J. M. Lopez-Soler, “Characteristics of Mobile YouTube Traffic,” *IEEE Wireless Comm.*, Feb. 2014.

Appendix A: Proof of Theorems in Chapter 3

A1 : Proof of Theorem 1 in Chapter 3

Denote $\{(\delta U^{(f)}, \delta G^{(f)}); 1 \le f \le F=V\times L\}$ to be the utility-resource pairs evaluated from all eligible (v, l) by Step1 of *VQD* method, where f is the rank index reflecting the sorted results of all $\eta_{v,l}$ in descending order, i.e. $\delta U^{(1)}/\delta G^{(1)} > \delta U^{(2)}/\delta G^{(2)} > \ldots > \delta U^{(F)}/\delta G^{(F)}$. Suppose J items are scheduled in total by Step 2 and assume

$$\delta U^{(1)}/\delta G^{(1)} > \delta U^{(2)}/\delta G^{(2)} > \ldots > \delta U^{(J)}/\delta G^{(J)} > \delta U^{(J+1)}/\delta G^{(J+1)}.$$

The index $J+1$ represents the first item not be selected due to insufficient slots, which means the following condition holds,

$$\delta G^{(J+1)} > G_0 - \sum_{f=1}^{J} \delta G^{(f)}. \tag{A.1}$$

Assume the *OPT* is the global optimal solution for **P1**, then

$$\sum_{f=1}^{J} \delta U^{(f)} + \delta U^{(J+1)} \ge OPT, \tag{A.2}$$

since the LHS has the largest unit utility gain. Denotes the solution obtained from *VQD* as OPT^{VQD}. The performance of *VQD* algorithm can be demonstrated in two phases:

<u>*Phase*-I</u>: In Step3, if an item f^* with the highest $\delta U^{(f^*)}$ results in

$$\delta U^{(f^*)} > \sum_{f=1}^{J} \delta U^{(f)},$$

where $J+1 \le f^* \le F$, OPT^{VQD}, can be expressed as

$$OPT^{VQD} = \delta U^{(f^*)} + \sum_{f'=1}^{J'} \delta U^{(f')} \ge \delta U^{(f^*)} > \sum_{f=1}^{j-1} \delta U^{(f)}, \tag{A.3}$$

where f' and J' is respectively the index of sorted result and the number of items scheduled after f^* is scheduled.

Since $\delta U^{(f^*)} > \sum_{f=1}^{J} \delta U^{(f)}$ and $\delta U^{(f^*)} \geq \delta U^{(J+1)}$, from (A.2), one has

$$OPT \leq \sum_{f=1}^{J} \delta U^{(f)} + \delta U^{(J+1)} \leq \delta U^{(f^*)} + \delta U^{(f^*)} = 2 \cdot \delta U^{(f^*)}.$$

Substituting (A.3) to above, we conclude

$$OPT \leq \sum_{f=1}^{J} \delta U^{(f)} + \delta U^{(J+1)} \leq 2 \cdot \delta U^{(f^*)} \leq 2 \cdot OPT^{VQD}. \tag{A.4}$$

This immediately implies $OPT^{VQD} \geq (1/2)\ OPT$ in *Phase*-I.

Phase-II*:* If there is no item f^* with highest $\delta U^{(f^*)}$, i.e. Step 3 is not triggered and , $\delta U^{(J+1)} \leq \sum_{f=1}^{J} \delta U^{(f)}$ by Step 4 and 5, we obtain

$$OPT^{VQD} = \sum_{f=1}^{J} \delta U^{(f)} - \delta U^{(i)} + \delta U^{(f")} \geq \sum_{f=1}^{J} \delta U^{(f)}, \tag{A.5}$$

where $\{\delta U^{(f")} > \delta U^{(i)}: 1 \leq i \leq J,\ J+1 \leq f" \leq F\}$.

Since $\delta U^{(J+1)} \leq \sum_{f=1}^{J} \delta U^{(f)}$, (A.2) becomes

$$\sum_{f=1}^{J} \delta U^{(f)} + \delta U^{(J+1)} \leq \sum_{f=1}^{J} \delta U^{(f)} + \sum_{f=1}^{J} \delta U^{(f)} = 2 \cdot \sum_{f=1}^{J} \delta U^{(f)}.$$

Substituting (A.5) into equation above we have

$$OPT \leq \sum_{f=1}^{J} \delta U^{(f)} + \delta U^{(J+1)} \leq 2 \cdot \sum_{f=1}^{J} \delta U^{(f)} \leq 2 \cdot OPT^{VQD} \tag{A.6}$$

This immediately leads to $OPT^{VQD} \geq (1/2)\ OPT$ in *Phase-II*, and (A.4) and (A.6) complete the proof of Theorem 1. ■

A2 : Proof of Theorem 2 in Chapter 3

For $1 \le f \le J$, $\delta U^{(f)}/\delta G^{(f)} > \delta U^{(J+1)}/\delta G^{(J+1)}$. Therefore,

$$\delta G^{(1)} \frac{\delta U^{(1)}}{\delta G^{(1)}} + \delta G^{(2)} \frac{\delta U^{(2)}}{\delta G^{(2)}} + ... + \delta G^{(J+1)} \frac{\delta U^{(J+1)}}{\delta G^{(J+1)}} \ \ge \ (\delta G^{(1)} + \delta G^{(2)} + ... + \delta G^{(J+1)}) \cdot \frac{\delta U^{(J+1)}}{\delta G^{(J+1)}}$$

$$\Rightarrow \delta U^{(1)} + \delta U^{(2)} + ... + \delta U^{(j)} \ \ge \ (\delta G^{(1)} + \delta G^{(2)} + ... + \delta G^{(J+1)}) \cdot \frac{\delta U^{(J+1)}}{\delta G^{(J+1)}}.$$

By applying (A.1), this inequation can be simplified as

$$\delta U^{(1)} + \delta U^{(2)} + ... + \delta U^{(J+1)} \ge G_0 \cdot \frac{\delta U^{(J+1)}}{\delta G^{(J+1)}}. \tag{A.7}$$

Since for all f, $\delta G^{(f)} \le \varepsilon G_0$, it follows from (A.7) that

$$\delta U^{(J+1)} \le \varepsilon \cdot (\delta U^{(1)} + \delta U^{(2)} + ... + \delta U^{(J+1)}) \le \frac{\varepsilon}{1-\varepsilon} \cdot (\delta U^{(1)} + ... + \delta U^{(J)}).$$

By using (A.2), it can be easily deduced that

$$(\delta U^{(1)} + \delta U^{(2)} + ... + \delta U^{(J)}) \ \ge (1-\varepsilon) \cdot OPT. \tag{A.8}$$

Recall that in (A.3) and (A.5), we already know that $OPT^{VQD} \ge \delta U^{(1)} + \delta U^{(2)} + \ldots + \delta U^{(J)}$ and applying it to (A.7). This completes the proof. It thus indicates that the OPT^{VQD} is extremely close to the OPT since the δG is very small as compared with the total UL slots G_0. ■

Vita

Po-Han Wu was born and grew up in Taipei, Taiwan. He received his Bachelor of Science degree in Mechanical Engineering from National Central University, Chungli, Taiwan, R.O.C. in 2002. He received his Master of Science degree in Electrical Engineering from Polytechnic University, New York (New York University Polytechnic School of Engineering now) in 2005.

He joined Information Processing Lab at University of Washington in 2006 and earned his Doctor of Philosophy degree in Electrical Engineering at University of Washington (UWEE) in 2014. He completed this half-year co-op in Network Data Planning Team of Verizon Wireless in 2012. After earning his master's degree, he flew back to Taipei to serve as a summer intern in Taiwan's Institute of Information Science of Academia Sinica until reporting to UWEE.

His research interests include multimedia network systems, OFDMA based mobile networks, real-time video transmission over wireless networks, optimization for wireless communication systems, video processing, and signal processing.